JCI The Journal of Clinical Investigation

BCL-2 antagonism sensitizes cytotoxic t cell-resistant hiv reservoirs to elimination ex vivo

Yanqin Ren, … , Catherine M. Bollard, R. Brad Jones

J Clin Invest. 2020. https://doi.org/10.1172/JCI132374.

Research In-Press Preview AIDS/HIV Immunology

Curing HIV infection will require the elimination of a reservoir of infected CD4+ T-cells that persists despite HIV-specific cytotoxic T-cell (CTL) responses. While viral latency is a critical factor in this persistence, recent evidence also suggests a role for intrinsic resistance of reservoir-harboring cells to CTL killing. This resistance may have contributed to negative outcomes of clinical trials, where pharmacologic latency reversal has thus far failed to drive reductions in HIV reservoirs. Through transcriptional profiling, we herein identified over-expression of the pro-survival factor BCL-2 as a distinguishing feature of $CD4^+$ T-cells that survived CTL killing. We show that the inducible HIV reservoir was disproportionately present in BCL-2^{hi} subsets, in ex vivo $CD4^+$ T-cells. Treatment with the BCL-2 antagonist 'ABT-199' alone was not sufficient to drive reductions in ex vivo viral reservoirs, when tested either alone or with a latency reversing agent (LRA). However, the triple combination of strong LRAs, HIV-specific T-cells, and a BCL-2 antagonist uniquely enabled the depletion of ex vivo viral reservoirs. Our results provide rationale for novel therapeutic approaches targeting HIV cure and, more generally, suggest consideration of BCL-2 antagonism as a means of enhancing CTL immunotherapy in other settings, such as cancer.

Find the latest version:

https://jci.me/132374/pdf

BCL-2 Antagonism Sensitizes Cytotoxic T Cell-Resistant HIV Reservoirs to Elimination *Ex Vivo*

Authors: Yanqin Ren[†1], Szu Han Huang[†1], Shabnum Patel[2,3], Winiffer D. Conce Alberto[1], Dean Magat[1], Dughan Ahimovic[1], Amanda B. Macedo[3], Ryan Durga[3], Dora Chan[3], Elizabeth Zale[1], Talia M. Mota[1], Ronald Truong[3], Thomas Rohwetter[3], Chase D. McCann[1], Colin M. Kovacs[4], Erika Benko[4], Avery Wimpelberg[5], Christopher Cannon[5], W. David Hardy[5,6], Alberto Bosque[3], Catherine M. Bollard[2, 3], R. Brad Jones[1,3]*

Affiliations:
[1]Infectious Diseases Division, Weill Cornell Medicine, New York, NY, USA.
[2]Childrens National Medical Center, Washington, DC, USA.
[3]Dept of Microbiology, Immunology, and Tropical Medicine, The George Washington University, Washington, DC, USA.
[4]Maple Leaf Medical Clinic, Toronto ON, Canada.
[5]Whitman-Walker Health, Washington, DC, USA.
[6]Division of Infectious Diseases, Johns Hopkins University School of Medicine, Baltimore, MD, USA

*** Corresponding author**: R. Brad Jones.
Email: rbjones@med.cornell.edu
Phone Number: (646)-962-2459
Mailing address: 413 East 69th Street, BB-526, New York, NY, 10021

Conflict of interest statement:
RBJ declares that he has received payments for his role on the scientific advisory board of AbbVie Inc. The other authors have declared that no conflict of interest exists.

Abstract

Curing HIV infection will require the elimination of a reservoir of infected $CD4^+$ T-cells that persists despite HIV-specific cytotoxic T-cell (CTL) responses. While viral latency is a critical factor in this persistence, recent evidence also suggests a role for intrinsic resistance of reservoir-harboring cells to CTL killing. This resistance may have contributed to negative outcomes of clinical trials, where pharmacologic latency reversal has thus far failed to drive reductions in HIV reservoirs. Through transcriptional profiling, we herein identified over-expression of the pro-survival factor BCL-2 as a distinguishing feature of $CD4^+$ T-cells that survived CTL killing. We show that the inducible HIV reservoir was disproportionately present in $BCL\text{-}2^{hi}$ subsets, in *ex vivo* $CD4^+$ T-cells. Treatment with the BCL-2 antagonist 'ABT-199' alone was not sufficient to drive reductions in *ex vivo* viral reservoirs, when tested either alone or with a latency reversing agent (LRA). However, the triple combination of strong LRAs, HIV-specific T-cells, and a BCL-2 antagonist uniquely enabled the depletion of *ex vivo* viral reservoirs. Our results provide rationale for novel therapeutic approaches targeting HIV cure and, more generally, suggest consideration of BCL-2 antagonism as a means of enhancing CTL immunotherapy in other settings, such as cancer.

Introduction

In the absence of antiretroviral treatment (ART), HIV maintains sustained viremia in most individuals, resulting in progression to AIDS. Several lines of evidence have established a role for $CD8^+$ T-cells in partially controlling viral replication, and delaying this progression (1-5). While a number of mechanisms contribute to this (6, 7), a key mode of action is the direct recognition and elimination of infected cells by $CD8^+$ cytotoxic T-cells (CTLs) (8, 9). Despite this antiviral activity, CTLs are not able to clear all HIV-infected cells from an individual, even when viral replication is abrogated by ART. This is generally attributed to viral latency, which leaves reservoirs of infected cells that invariably re-establish systemic viremia if ART is ever interrupted (10-12).

The "kick-and-kill" (or "shock-and-kill") paradigm proposes to combine latency-reversing agents (LRAs) to induce HIV antigen expression, with immune effectors, such as CTLs, to eliminate infected cells from the reservoir (13, 14). Although kick-and-kill approaches have proven effective *in vitro* against primary cell models of latency, they have thus far failed to drive measurable reductions in frequencies of infected cells in clinical trials (15-20). In an effort to bridge these contrasting results, we have focused on evaluating kick-and-kill approaches against $CD4^+$ T-cells derived directly *ex vivo* from ART-suppressed individuals. We previously reported that we were unable to drive reductions in viral reservoirs from these samples, as measured by quantitative viral outgrowth assays (QVOA), despite the use of potent LRAs, and functional CTLs targeting non-escaped viral epitopes (21). In those experiments, we recovered virus from QVOA wells, super-infected autologous $CD4^+$ T-cells, and demonstrated that the same CTLs that had been unable to eliminate the latent reservoir efficiently eliminated cells newly infected with these reservoir viruses. These results argued against viral escape or CTL dysfunction as mechanisms by which these reservoirs were not eliminated *ex vivo*, and led us to propose that reservoir-harboring cells from ART-suppressed individuals are resistant to elimination by CTLs (22). Of note, a separate study has recently shown that virus derived from clonally-expanded HIV-infected cells from ARV-treated individuals often remains sensitive to autologous CTL, further arguing against epitope escape as a dominant mechanism underlying the persistence of these cells (23).

Natural heterogeneity is known to exist in the intrinsic susceptibility of $CD4^+$ T-cells to killing by CTL, supporting the plausibility of a reservoir that has been selected to be CTL resistant. For example, central memory $CD4^+$ T-cells are more resistant than transitional and effector memory subsets, and activated $CD4^+$ T-cells are more susceptible than their resting counterparts (24). One study has also reported that $CD4^+$ T-cells from HIV-positive individuals who exhibit natural control of viral replication are intrinsically more sensitive to killing than those from individuals with progressive disease, suggesting a role for the susceptibility of these cells to CTL killing in disease outcome (25). The mechanism for these differential

susceptibilities of $CD4^+$ T-cell subsets to CTL-mediated elimination is unclear, though multiple mechanisms of resistance have been identified in other cell types (26-29).

To address the challenge of CTL resistance, we performed RNA sequencing (RNAseq) transcriptional profiling of peptide-pulsed primary $CD4^+$ T-cells that preferentially survived co-culture with corresponding HIV-specific CTL. We identified a number of genes and pathways that were differentially regulated in survivors, including over-expression of the pro-survival factor BCL-2, which we selected for further study. CTL-mediated elimination of target cells occurs when the TCR binds its cognate peptide-MHC-I complex, triggering the release of perforin/granzymes, or through Fas/FasL interactions (30). BCL-2 (B-cell lymphoma 2) is a master regulator of apoptosis that can inhibit both the perforin/granzyme B and FasL/Fas pathways by sequestering Bid, thus preventing mitochondrial membrane permeabilization by tBid (30-34). We show that cells harboring the inducible HIV reservoir express high levels of BCL-2 following *ex vivo* reactivation. In the oncology setting, the pro-survival BCL-2 family proteins have been identified as key factors in the resistance of many tumor cells to death (35-38). BCL-2 antagonists, such as ABT-199 (venetoclax), have been developed as cancer therapies which aim to directly promote the apoptosis of tumor cells, which often over-express BCL-2 (35-40). By adding ABT-199 to our "kick-and-kill" co-cultures, we were able to achieve the reductions in *ex vivo* HIV reservoirs that we have been unable to achieve with CTL and LRAs alone. This has direct implications for efforts to eliminate persistent HIV reservoirs, and may contribute to our understanding of potential CTL-dependent mechanisms of action of BCL-2 antagonists in other settings, such as cancer.

Results

Transcriptional Profiling of Target $CD4^+$ T-cells that Survive CTL Co-culture Reveals Candidate Mechanisms of Resistance

To identify candidate mechanisms that may confer CTL resistance to HIV reservoir harboring cells, we first studied differential intrinsic sensitivities to CTL killing in primary $CD4^+$ T-cells. Given that different maturational phenotypes of $CD4^+$ T-cells are associated with differential susceptibilities to CTL (24), we sought to minimize this variable by synchronizing target cells in a central memory (T_{CM}) phenotype, as these cells preferentially harbor the latent reservoir (41). This was achieved following the protocol used to generate cells for the 'cultured T_{CM} model' of HIV latency (see Supplementary Methods) (42, 43). T_{CM} cells were divided into either a "real" condition, where half of the cells were labeled with CFSE and pulsed with the HIV-Env peptide RLRDLLLIVTR, while the other half received no peptide and were labeled with CTFR, or a "mock" condition where cells were similarly labeled but received no peptide. Both conditions were then co-cultured with the corresponding CTL clone **(Fig. 1A).**

This design allowed the isolation of transcriptional profiles associated with preferential survival from profiles that resulted from exposure to an environment containing activated CTL, i.e: **i**) the 'mock bystanders' and 'mock survivors' should not differ from each other **ii**) the difference between either 'mock bystanders' or 'mock survivors' and 'real bystanders' should reflect exposure of the latter to peptide-stimulated CTL (ex. cytokine signaling), **iii**) the difference between 'real bystanders' and 'real survivors' should reflect selection for factors that confer CTL resistance, and **iv**) the difference between 'real survivors' and either of the mock conditions should reflect a combination of **ii** and **iii** (**Fig. 1A**). Following an overnight co-culture, $CD4^+$ T-cells in both conditions were sorted into 'bystanders' (CTFR) and 'survivors' (CFSE) populations by flow cytometry, and subjected to transcriptional profiling by RNA sequencing (RNAseq).

Principal component analysis (PCA) of the resulting RNAseq data revealed a pattern that was consistent with the above expectations, with the 'mock bystanders' and 'mock survivors' clustering together, while the 'real survivors' and 'real bystanders' formed distinct clusters (**Fig. 1B**). As expected, the differences between the 'real bystanders' and the 'mock bystander' conditions were predominately attributable to the former having been co-cultured with peptide-stimulated CTL – ex. cytokine signaling, interferon signaling,

and T-cell activation (**Fig. S1A**). Of greater importance to the current study, the comparison between the 'real survivors' and 'real bystanders' identified 1,061 differentially expressed genes (DEGs) FDR<0.05: 743 upregulated and 318 downregulated. Ingenuity Pathway Analysis (IPA) was performed, and the significantly enriched pathways are shown in **Fig. 1C** (B-H Multiple Testing Correction p-value<0.05). A number of individual genes appeared multiple times in these pathways, as indicated in **Fig. 1D**. To further identify key genes, and establish connections between these, we generated gene network diagrams based on the ingenuity pathway knowledge base (IPKB). Amongst these networks, we highlight one which contains components of the following canonical pathways relevant to our hypothesis: Cytotoxic T Lymphocyte-Mediated Apoptosis of Target Cells, Death Receptor Signaling, Interferon Signaling, and Mitochondrial Dysfunction (**Fig. 1E**). This 'network 6', and all other networks are listed in **Table S1**, along with scores**.** Following from this result, we assessed the expression levels of the genes implicated in the 'cytotoxic T lymphocytes-mediated apoptosis of target cells' pathway (caspase-2 and BCL2), as well as PARP, a mediator of apoptosis that is downstream of caspase activation. We observed expression profiles that were consistent with specific selection of over-expression of BCL2, and under-expression of caspase-2 and PARP in the 'real survivor' cells that resisted elimination by CTL (**Fig. 1F**). These results confirm that heterogeneity exists in the intrinsic sensitivity of $CD4^+$ T-cells to elimination by CTL, and is associated with a transcriptional signature implicating multiple gene pathways. We prioritized BCL2 for validation and further study based on its central position within the network shown in **Fig. 1E**, its central role in cell survival, and its potential to directly antagonize killing by CTL (30-34).

HIV-specific CTLs Preferentially Kill BCL-2^{lo} Primary $CD4^+$ T-cells, thus Selecting for BCL-2^{hi} Survivors in vitro

We next determined if the over-expression of BCL2 transcripts observed in RNAseq data was reflected at the protein level, with the hypothesis that BCL-$2^{hi}CD4^+$ T-cells would preferentially survive CTL-mediated killing. We tested this by co-culturing HIV-Specific CTLs with autologous $CD4^+$ T-cells that had been

pulsed with various concentrations of its cognate peptide, and measuring BCL-2 expression levels in surviving $CD4^+$ T-cell **(Fig. 2A-B)**. We observed significant losses in viable $CD4^+$ T-cells with increasing peptide concentrations (10μg/mL peptide vs NoTx, 3.2-fold decrease $p<0.0001$; 2.1-fold decrease vs 0.01μg/mL peptide, $p<0.0001$, **Fig. 2C**), and a corresponding increase in BCL-2 expression in the remaining $CD4^+$ T-cells (10μg/mL vs NoTx, $p=0.008$; vs 1μg/mL, $p=0.03$, **Fig. 2C&D)**. This effect was confirmed by assessing the impact of CTL killing on total numbers of target cells as divided into BCL-2^{hi} and BCL-2^{lo} populations **(Fig. 2E)**. We observed a progressive decrease in the numbers of BCL-2^{lo} cells with increasing peptide concentrations (mean count – 83,000 at 0.01μg/mL peptide vs. 45,000 at 10μg/mL peptide, $p=0.009$, **Fig. 2E**), alongside a lack of significant change in the numbers of BCL-2^{hi} cells, even at 10μg/mL of RR11 peptide (**Fig. 2E)**. Thus, these data support that the natural heterogeneity of BCL-2 expression within *ex vivo* $CD4^+$ T-cells is sufficient to influence susceptibility to CTL killing, with BCL-2^{hi} cells exhibiting preferential survival. This association could either reflect differences across maturational phenotypes – where, for example, naïve $CD4^+$ T-cells may both express lower levels of BCL-2 and be more susceptible to CTL killing – or, may also reflect heterogeneity of these parameters within a given phenotype. To distinguish between these, we performed a similar killing assay as in **Fig. 2E**, with the addition of phenotypic marker staining to discriminate naïve – $CD45RA^+CCR7^+$, central memory (CM) – $CD45RA^-CCR7^+$, and effector memory (EM) – $CD45RA^-CCR7^-$ populations. Parallel experiments were performed where cells were either activated with anti-CD3/anti-CD28 prior to peptide pulsing and co-culture, or were peptide pulsed without prior activation. We observed the preferential survival of BCL-2^{hi} cells within each of these populations, whether or not cells had been activated (**Fig. 2F**). The most pronounced skewing in BCL-2 expression was observed within the T_{EM} cells (**Fig. 2F**), which corresponded with a greater degree of killing of this population (%killed at 5 μg/ml peptide by phenotype: T_{CM} – 21.7%, T_{EM} – 63.9%, naïve – 36.8%). Thus, even within a given maturational population, the relative expression of BCL-2 is associated with susceptibility to elimination by CTL.

The Reactivatable HIV Reservoir is Preferentially Harbored in BCL-2^{hi} Cells in Individuals on Long-Term ART

Given the above observations that BCL-2^{hi} cells preferentially resist killing by CTL, we next probed a potential role for this mechanism in the persistence of the HIV reservoir. We first assessed BCL-2 expression levels in *ex vivo* CD4$^+$ T-cells from ART-suppressed donors, following latency reversal with PMA/Ionomycin (PMA/I) (**Fig. 3A**). This was accomplished using a recently developed flow cytometry technique which allows for the identification and phenotypic characterization of this extremely rare population (44). We established a gating strategy using cells from an ART-naïve, chronically HIV-positive individual ('OM5374') and an HIV-negative donor ('OM6960') (**Fig. 3A**). As expected, we observed a lack of Gag$^+$ cells in the HIV-negative sample, contrasted by a detectable population in the HIV-positive sample, which was enhanced by PMA/I stimulation.

We extended this assay to measure differences of BCL-2 expression levels between HIV-infected and uninfected cells amongst *ex vivo* CD4$^+$ T-cells from 6 additional durably ART-suppressed study participants (**Table 1**). We observed extremely rare HIV-infected populations from each participant following PMA/I stimulation, while no Gag$^+$ events were observed in unstimulated cells (**Fig. 3B**). For each individual, HIV-Gag$^+$ populations were found to express higher levels of BCL-2 (MFI 2874, range: 1460–5820) than corresponding Gag$^-$ populations (MFI 1215, range: 1100-1320) (p=0.01, **Fig. 3C-D**). In contrast to these ART-suppressed individuals, we observed similar BCL-2 expression levels between the Gag$^+$ (MFI mean: 1,001, range: 965-1,450) and Gag$^-$ cell populations (MFI mean: 1,007, range: 1,093-1,350) from 4 ART-naïve participants (**Table 2)**, following PMA/I stimulation **(Fig. 3E-F)**. Although we acknowledge inherent limitations of analyzing such very rare events, we draw confidence in our conclusion from the observation that this difference was statistically robust across a cohort of 6 individuals (p=0.016, **Fig. 3D**). Thus, we observed that, following reactivation, the HIV reservoir in ART-suppressed individuals capable of producing Gag is preferentially present in BCL-2^{hi} cells. This suggests that the levels of BCL-2 over-

expression from ARV-treated individuals are not simply the result of HIV expression, but rather may be a feature that is enriched in cells comprising long-lived HIV reservoirs.

As an additional method for assessing the BCL-2 expression profile of reservoir-harboring cells, we sorted *ex vivo* $CD4^+$ T-cells from long-term ART-suppressed individuals into BCL-2^{hi} and BCL-2^{lo} populations by flow cytometry, and quantified HIV DNA in each population. HIV DNA was measured using a recently developed droplet digital PCR method that allows for the discrimination of relatively intact proviruses, which contain binding sites for both *gag* and *env* primer/probe pairs (45). We observed significantly higher frequencies of HIV proviruses in BCL-$2^{hi}CD4^+$ T-cells, compared to BCL-2^{lo} population ($p=0.02$ for "intact" and total *gag*) (**Fig. 4A**). We next determined whether this enrichment of infected cells in the BCL-2^{hi} subset was reflective of differences across maturational populations, or whether BCL-2^{hi} cells would be enriched for infected cells even within a given memory population. We included the maturational markers CCR7 and CD45RA in our flow cytometry panel, and sorted cells from two donors into BCL-2^{hi} and BCL-2^{lo} subsets for each: of naïve – $CD45RA^+CCR7^+$, central memory (CM) – $CD45RA^-CCR7^+$, and effector memory (EM) – $CD45RA^-CCR7^-$ populations (**Fig. 4B**). For both individuals, we observed pronounced enrichments of "intact" HIV DNA in the BCL-2^{hi} vs BCL-2^{lo} populations. These patterns were also reflected at the level of total HIV DNA in each memory subset (**Fig. 4C**). These data provide an additional line of evidence supporting that the HIV reservoir is preferentially harbored in BCL-2^{hi} cells in individuals on long-term ART, and indicate that this is not merely reflective of differences across maturational phenotypes.

BCL-2 Antagonist ABT-199 Fails to Reduce Either Total HIV DNA or Infectious Reservoirs from ex vivo $CD4^+$ T-cells from ARV-Treated Donors, but can Drive Reductions in a Primary Cell Latency Model

A previous study reported that the combination of ABT-199 with anti-CD3/anti-CD28 antibodies was sufficient to drive reductions in the frequencies of HIV-infected cells taken *ex vivo* from ART-suppressed participants (46). However, this was not associated with reductions in the amounts of HIV RNA released

into culture supernatants, and the effect on the inducible infectious reservoir as measured by QVOA was not tested. As a prelude to assessing the abilities of ABT-199 to sensitize HIV reservoir-harboring cells to elimination by CTL, we therefore determined whether this agent had activity against latently HIV-infected cells when used either alone, or in combination with a LRA.

In our experiments, the effects of BCL-2 antagonist ABT-199 were assessed using an HIV eradication (HIVE) assay (**Fig. 5A**), where changes in infected cells are measured by both droplet digital PCR (ddPCR) to measure total frequencies of infected cells (total HIV DNA), and QVOA to measure replication competent reservoirs (infectious units). This distinction is important as, in *ex vivo* $CD4^+$ T-cells from ARV-treated individuals, the large majority of HIV DNA represents defective proviruses with no potential for viral replication (47). In our HIVE assays, we focused on the protein kinase C agonist bryostatin-1 as the LRA, as we had observed that it mitigated the appreciable levels of non-specific $CD4^+$ T-cell toxicity induced by ABT-199 (**Fig. S2**). Potent activation of $CD4^+$ T-cells by bryostatin-1 was confirmed by CD69 staining (**Fig. S3**). We were careful to account for cell death in our QVOAs by counting only viable $CD4^+$ T-cells by flow cytometry following a 24-hour drug wash-out period to calculate infectious units per million $CD4^+$ T-cells (IUPM). We further confirmed that prior treatment with ABT-199 did not continue to negatively affect viability after the 24-hour wash-out, which may have otherwise introduced inaccuracy into our QVOA measurements (**Fig. S4**). DNAse I was also included in the HIVE co-culture medium to degrade the genomes of killed target cells such that these would not be measured by ddPCR.

We first tested whether ABT-199 would drive reductions when targeting 'natural' HIV reservoirs in *ex vivo* $CD4^+$ T-cells from ART-suppressed donors. A representative example of a HIVE assay is shown in **Fig. 5B**. We did not observe reductions in either HIV DNA or IUPM following treatment with ABT-199 (1μM or 100nM), either alone or in combination with bryostatin-1 (**Fig. 5B**). In this initial experiment, the overall loss in viability meant that we had insufficient cells to assess conditions treated solely with ABT-199 (1μM)

by QVOA. The only significant differences that we observed were increases in IUPM following treatment with bryostatin-1 alone ($p<0.001$, **Fig. 5B**). We extended this HIVE assay to a total of 8 ARV-treated donors, and consistently observed a lack of significant differences in either HIV DNA or IUPM between untreated conditions and ABT-199 (both 1μM and 100nM), tested either alone or in combination with bryostatin-1 (**Fig. 5C-D**). In contrast, the increases in IUPM observed with bryostatin-1 treatment were found to be consistent across this population ($p<0.01$ at 1μM, and $p=0.03$ at 100nM, **Fig. 5C-D, right columns**). Thus, the BCL-2 antagonist ABT-199 was not sufficient to drive reductions in *ex vivo* viral reservoirs – including when combined with the potent LRA bryostatin-1. Although peripheral to the main hypothesis of the current study, we were curious to see if this combination would be sufficient to drive the elimination of infected cells in a well-characterized primary cell model of HIV latency (48, 49). This model typically harbors ~1% latently-infected cells that can be reactivated to produce HIV by anti-CD3/anti-CD28. This frequency is much too high to be measured by a typical QVOA, which is designed to detect infected cell frequencies of ~0.00001 – 0.001%. Thus, to enable direct comparison to our results from 'natural' HIV reservoirs, we generated target populations with reduced infected-cell frequencies by spiking latency model cells into autologous $CD4^+$ T-cells at ratios of 1 model cell:100-1,000 *ex vivo* $CD4^+$ T-cells (**Fig. S5A**). In contrast to 'natural' HIV reservoirs, we observed that ABT-199 (1μM and 100nM), alone or in combination with bryostatin-1, drove reductions in latency model cells as measured either by ddPCR or QVOA (**Fig. S5**). Most strikingly, we observed a 130-fold reduction in IUPM in the bryostatin-1+1μM ABT-199 condition ($p<0.0001$), and a 21-fold reduction in IUPM in the bryostatin-1+100nM ABT-199 condition ($p<0.0001$, **Fig. S5B**). Our results are consistent with a previous study which also reported infected-cell reductions in a latency model following treatment with ABT-199 and anti-CD3/anti-CD28 (as an LRA) (46). These spiked latency model HIVEs also offer validation both for our treatment conditions, and confirm our ability to measure changes in the reservoir in HIVE assays. Thus, our results firmly establish that – while effective against a latency model – ABT-199 in combination with the LRA bryostatin-1 was insufficient to reduce HIV reservoirs *ex vivo*.

Combinations of a Potent Latency Reversing Agent, HIV-specific CTL, and a BCL-2 Antagonist Drive Reductions in HIV Reservoirs from ex vivo CD4$^+$ T-cells

In our hands, both combinations of LRA+ABT-199 and of LRA+CTL were individually effective against primary cell latency models, but not against *ex vivo* reservoirs. We therefore next tested the central hypothesis of the current study, that a combination of these treatments would deplete *ex vivo* reservoirs as a result of ABT-199 counteracting resistance to CTL-mediated elimination **(Fig. 6A).** In an initial experiment, using cells from an ARV-treated donor 'OM5011' (see **Table 1**), we continued to utilize bryostatin-1 as an LRA, and measured the elimination of latently-infected cells with ddPCR – quantifying HIV DNA at both *gag* and *env* amplicons. Using two different autologous HIV-Gag-specific CTL clones (targeting the ACQGVGGPGHK 'AK11' and the HPVHAGPIA 'HA9' epitopes), we observed significant depletions in HIV DNA as measured at the *env* target sequence uniquely in the triple combination condition of bryostatin-1+Gag-specific CTL+ABT-199 (both $p<0.01$ respectively, **Fig. 6B**). We included an autologous CMV-pp65-specific CTL clone as an additional control, and observed a lack of depletion in HIV DNA, as expected (**Fig. 6B**). Using samples from the same experiment, we observed non-significant trends towards depletion in HIV DNA as measured at the *gag* target sequence for both CTL conditions (AK11 – $p=0.20$, HA9 – $p=0.15$, **Fig. 6C**). In a second experiment, we utilized an autologous polyclonal HIV-specific T-cell products that has been developed for T-cell therapy (termed "HSTs") (50, 51). The HSTs used in this study (**Fig. 6D&E, and Fig. 7&8**) exhibited high frequencies of HIV-specific T-cells (IFN-γ responses to HIV-Gag/Nef/Pol peptide pools, range: 6970–28,130 SFC/10^6 cells), and they were confirmed to respond to multiple epitopes by ELISPOT and intracellular cytokine staining (**Fig. S6A-C**), and exhibited strong cytotoxicity against peptide-pulsed cells (**Fig. S6D)**. In this experiment, we observed that the triple combination of bryostatin-1+HSTs+ABT-199 uniquely drove a significant reduction in HIV DNA, as measured by primers and probes targeting *gag* (**Fig. 6D)**, however a trend towards a reduction in ddPCR targeting *env* did not reach statistical significance ($p=0.06$, **Fig. 6E**). While these initial results did

provide some support for our hypothesis, we also considered them to be somewhat marginal due to the lack of consistent statistical significance. Given how resource intensive these HIVE assays are (ex. using ~1 x 10^9 PBMCs per donor per experiment), we opted to transition to the use of the "maximally activating" LRA anti-CD3/anti-CD28 for HIVE assays, positing that this would enhance our ability to detect an ability of ABT-199 to sensitive reservoir-harboring cells to elimination by kick and kill.

We assessed the combination of anti-CD3/anti-CD28, ABT-199, and autologous HSTs in an initial HIVE assay targeting *ex vivo* $CD4^+$ T-cells from ART-suppressed donor OM5148. The elimination of reservoir-harboring cells was measured in parallel by ddPCR, and QVOAs (**Fig. 7A**). We observed significant reductions in total HIV DNA (**Fig. 7B-C)** following treatment with anti-CD3/anti-CD28 and HSTs, as well as with anti-CD3/anti-CD28 and ABT-199, and further significant reductions with anti-CD3/anti-CD28+HSTs+ABT-199 (**Fig. 7B,** 3.4-fold vs. NoTx, $p<0.0001$; 2.1-fold vs. anti-CD3/anti-CD28+HSTs, $p=0.009$; 1.9-fold vs. anti-CD3/anti-CD28+ABT-199, $p=0.03$). Consistent with our previous work, the decrease in HIV DNA with a maximal LRA+T-cells was not mirrored by a decrease in levels of replication competent provirus as measured by QVOAs. Only by combining ABT-199 with anti-CD3/anti-CD28+HSTs, we were able to observe a significant reduction in this infectious reservoir, with no $p24^+$ wells observed in the QVOA (IUPM 0 vs. NoTx:0.66, $p=0.02$, **Fig. 7D**). We next performed an analogous HIVE using an autologous HIV-specific CTL clone targeting a non-escaped HIV epitope, which had previously failed to eliminate 'natural' HIV reservoirs in the absence of ABT-199 (21). As before, treatment with anti-CD3/anti-CD28+CTL led to significant 2.1-fold reductions in HIV DNA, while further significant 5.7-fold reductions were observed with anti-CD3/anti-CD28+CTL clone+ABT-199 (**Fig. 7C**). However, significant decreases in IUPM were uniquely observed with the triple combination of anti-CD3/anti-CD28, CTL clones, and ABT-199 (0.32 vs. 2.63 NoTx, $p<0.001$, **Fig. 7E).** Thus, in two initial HIVE assays using either HSTs or a CTL clone, we observed that ABT-199 facilitated reductions in IUPM that were not observed with effectors+LRA without ABT-199.

We next tested these treatment conditions in 8 additional HIVE assays, using *ex vivo* $CD4^+$ T-cells from 7 participants. For three HST-based HIVE assays, we also ran separate matched HIVE assays using autologous HIV-specific CTL clones confirmed to target non-escaped epitopes (indicated by red lines**, Fig. 8);** CTL clones, along with HSTs, are collectively referred to hereafter as HIV-spec. effectors. As in the above experiments, we observed appreciable non-specific cell toxicity in the ABT-199-treated conditions. This was accounted for in all HIVE assays by applying only viable $CD4^+$ T-cell counts when plating QVOAs and calculating IUPM (**Fig. S7)**. In HIVE assays where we were unable to recover >3 million viable cells, all cells were plated in QVOAs to maximize the accuracy of our IUPM calculations, without a matched measurement for HIV DNA. Summary data for HIV DNA showed no significant decreases following treatment with anti-CD3/anti-CD28 alone or with anti-CD3/anti-CD28+ABT-199 (p=0.16 and p=0.23 respectively, **Fig. 8A**). Treatment with anti-CD3/anti-CD28+HIV-specific effectors led to overall significant decreases in HIV DNA (p=0.02), which were also observed with the addition of ABT-199 (p=0.03, **Fig. 8A).** In terms of intact-inducible reservoirs, QVOA results showed no significant decreases in IUPM when comparing the NoTx condition to either of: anti-CD3/anti-CD28, anti-CD3/anti-CD28+ABT-199, or anti-CD3/anti-CD28+HIV-spec. effectors (**Fig. 8B)**. However, when cells were treated with the triple combination of anti-CD3/anti-CD28, HIV-spec. effectors, and ABT-199, we observed significant decreases in IUPM compared to the NoTx condition (p=0.03, **Fig. 8B**). When considered individually, as in **Fig. 7D&E**, decreases in QVOA were also significant for 9/10 HIVE assays following treatment with the triple combination. Differences in IUPM were also significant when directly comparing anti-CD3/anti-CD28+ABT-199 to the triple combination of anti-CD3/anti-CD28+HIV-spec effectors+ABT-199 (p=0.02, **Fig. 8D**). In conclusion, while cells harboring intact-inducible HIV reservoirs - as measured by QVOA - were not reduced following treatment with anti-CD3/anti-CD28 and either ABT-199 or HIV-specific T-cell effectors, the combination of all three treatments unlocked consistent reductions in viral reservoirs in *ex vivo* $CD4^+$ T-cells from ART-suppressed individuals.

Discussion

The interaction with a CTL that results in target cell elimination is a highly regulated process on the part of both cells. In the context of HIV, the factors that define an effective CTL have been the subject of considerable study, which has led to numerous key insights such as the role of T-cell exhaustion in limiting immune control of viral replication (7, 52-56). In contrast, little is known about how intrinsic differences in infected-cell sensitivity may influence the outcome of interactions with CTL. The potential importance of this consideration is highlighted by oncology studies where intrinsic resistance to CTL on the part of target cells has emerged as a key factor limiting the efficacy of immunotherapies (57, 58). In a recent study, we highlighted the potential role of intrinsic target cell resistance to CTL killing in HIV persistence. In the current study, we provide evidence for a causal role for BCL-2 in this resistance by demonstrating that a selective BCL-2 antagonist, ABT-199, enabled reductions in *ex vivo* infectious reservoirs following latency reversal and co-culture with HIV-specific T-cells. The transcriptional profiling performed here has also identified additional candidate mechanisms of resistance that will be pursued in future studies.

Our data with *ex vivo* $CD4^+$ T-cells indicate that ABT-199 acted by enabling CTL killing, since significant reductions were not observed with either LRA+CTL, or with LRA+ABT-199. However, this must be contextualized within a more complex landscape, given that BCL-2 antagonism can also drive apoptosis through CTL-independent mechanisms (59-61). Overall, we interpret the results of our study to indicate that ABT-199 contributed to cell death by three mechanisms, depending on the source and infection status of the target cells. First, we consistently observed appreciable losses in the overall viability of both *ex vivo* and latency model cells, independent of any CTL recognition – likely as a result of an overall skewing of the anti-/pro-apoptotic balance maintained by BCL-2. This non-specific induction of apoptosis was substantially mitigated by bryostatin-1, which is known to suppress apoptosis by phosphorylating and thus activating BCL-2 (62), and to a lesser degree by anti-CD3/anti-CD28 stimulation. We took care to control

385 for any confounding effects arising from this non-specific toxicity by calculating IUPM values based on
386 only viable $CD4^+$ T-cells in each experimental condition. Second, in the T_{CM} primary cell latency model,
387 we observed dramatic reductions in relative frequencies of HIV-infected cells following treatment with
388 ABT-199 (in the absence of CTL); indicating that HIV-infected cells were disproportionately susceptible
389 to ABT-199-induced apoptosis as compared to uninfected cells. This result can be explained by recent
390 publications showing that Casp8p41 binds with BCL-2 in HIV-infected cells, which averted cell death (63).
391 The BCL-2 antagonist ABT-199 can release Casp8p41 and specifically enhance the susceptibility of HIV-
392 infected cells to viral cytopathicity (64). Interestingly, and in contrast to results from this latency model,
393 viral cytopathicity did not appear to be sufficient to drive the death of reservoir-harboring cells from *ex vivo*
394 $CD4^+$ T-cells, even in the presence of ABT-199. Rather, ABT-199 facilitated the death of *ex vivo*, HIV-
395 infected cells by a third, CTL-dependent mechanism, consistent with the central hypothesis of the current
396 study.
397
398 The mechanisms underlying our observation that infected cells in a primary cell latency model were
399 susceptible to elimination by ABT-199+LRA, whereas those in *ex vivo* $CD4^+$ T-cells were not, are currently
400 unknown. However, these results appear to mirror our prior inability to reduce infectious reservoirs with
401 combinations of CTL and LRAs; whereas such combinations are effective against models of latency (13,
402 21, 65). We suggest that these results fit an emerging pattern in the field, as also evident in unsuccessful
403 clinical trials, supporting the idea that HIV reservoir-harboring cells - which durably persist in individuals
404 on long-term ART - possess a resiliency that may not be reflected in short-term *in vitro* models of latency
405 (22). The results of our study suggest one mechanism by which such resiliency could emerge - through
406 infection of $CD4^+$ T-cells possessing natural variation in BCL-2 activity, followed by *in vivo* selection of
407 an apoptosis resistant $BCL\text{-}2^{hi}$ population. Initial support for this hypothesis is present in our observation
408 of similar BCL-2 expression levels between Gag^+ and Gag^- cells in *ex vivo* $CD4^+$ T-cells from 4 ART-naïve
409 individuals, in comparison to elevated BCL-2 expression in Gag^+ cells from individuals on long-term ART.
410 In the ART-naïve samples, the majority of *ex vivo* Gag^+ cells will have been newly infected with HIV and

411 would have been destined to die shortly after this snapshot – with an average lifespan of ~2.2 days (66). In
412 contrast, the infected cells reactivated from individuals on ART represent long-term survivors that were
413 almost certainly infected prior to ART initiation (years prior). Recently, it has been demonstrated that the
414 HIV reservoir is dynamically shaped by the proliferation and contraction of clones of HIV-infected cells
415 (67), providing the replication and heritability needed to drive evolution within this surviving population,
416 and the selection of pro-survival factors, such as BCL-2. A broader rendering of this hypothesis would
417 include not only BCL-2, but other factors which influence the susceptibility of cells to apoptosis. One such
418 factor is the anti-apoptotic protein BIRC5 (survivin) - the expression of which was recently demonstrated
419 to be over-represented in clonally expanded cells in *ex vivo* $CD4^+$ T-cells (68). Such CTL-driven selection
420 would be dependent upon the expression of antigen, and thus one may think that it would uniquely apply
421 to cells harboring intact proviruses, and not to those with defective proviruses. However, the dichotomy of
422 intact proviruses being associated with antigen expression, while defective proviruses are not, does not fully
423 reflect the complexity of the proviral landscape. A subset of defective proviruses are capable of expressing
424 antigen, and thus of being recognized by CTL (69, 70). On the other hand, a large proportion of intact
425 proviruses are not expressed, even following stimulation with maximal LRAs, and thus are unlikely to
426 express antigen *in vivo*. We suggest that this complexity underlies our observations that – whereas for some
427 individuals only 'intact' proviruses were enriched in BCL-2^{hi} cells (ex. WWH-B011 in **Fig. 4C**), in other
428 individuals a degree of enrichment was also observed for total HIV DNA (mostly defective) (**Fig. 4A**). We
429 also note that whereas BCL-2 antagonism was required to achieve measurable reductions in QVOA assays,
430 it did also further enhance CTL-mediated reductions in total HIV DNA (**Fig. 7B &C**), further supporting
431 that a subset of defective proviruses are harbored from CTL in BCL-2^{hi} cells. Additional longitudinal
432 studies of the expression of BCL-2 and other survival factors in *ex vivo* reservoir-harboring cells are needed
433 to further test the hypothesis that CTL select for infected cells with these pro-survival phenotypes. Pairing
434 such studies with profiling of proviral landscapes and integration sites would allow further scrutiny of this
435 hypothesis, by assessing whether such selection is limited to cells harboring proviruses that are likely to
436 drive antigen expression.

The results of our study suggest the possibility of adding BCL-2 antagonist to therapeutic combinations of CTL and LRAs with the aim of achieving the *in vivo* reductions in HIV reservoirs that have eluded clinical trials to date. The BCL-2 antagonist ABT-199 used in the current study is the active ingredient in the licensed drug Venclexta® (venetoclax), which is used to treat chronic lymphocytic leukemia (CLL)(71). Although Venetoclax has non-trivial side-effects, it is reasonably well-tolerated, with CLL patients often taking this drug for years (72). It is therefore worth considering clinical trials involving BCL-2 antagonist as a possible strategy for reducing or eliminating HIV reservoirs in individuals on long-term ART. As our *ex vivo* results suggest that the co-ordination of these agents with HIV-specific CTL may be needed to achieve such reductions, it is important to note that ABT-199 did not impair the viability or functionality of $CD8^+$ T-cells [see also (73)]. Moreover, in a murine cancer model, Venetoclax enhanced anti-PD-1 mediated T-cell anti-tumor activity (73, 74). In conclusion, the current study provides evidence that HIV reservoir-harboring cells have been selected for survivability, conferred – at least in part – through BCL-2. This establishes a rationale for the development of novel tripartite therapies incorporating latency reversing agents, BCL-2 antagonism, and enhancement of $CD8^+$ T-cell responses through immunotherapy, cell therapy, or vaccination to reduce or eliminate HIV reservoirs.

Methods

Agents: Latency reversing agents, Chemical agents and Antibodies

LRAs and BCL-2 antagonist were used at the following concentrations: Bryostatin-1 dissolved in DMSO at 10nM (Sigma-Aldrich); anti-CD3 (OKT3, Biolegend), anti-CD28 (CD28.2, Biolegend) anti-CD3/anti-CD28 antibodies were used at 1μg/mL each; PMA and Ionomycin were dissolved in DMSO, and PMA was used at 25nM (Sigma-Aldrich), Ionomycin at 1μg/ml (Sigma-Aldrich); ABT-199 (Med Chem Express,

Cat# HY-15531) was dissolved in DMSO used at 1μM or 100nM (as indicated). Fixable viability dye (aqua, ThermoFisher), anti-human CD3 (clone SK7, BD Biosciences), anti-human CD4 (clone RPA-T4, BD Biosciences), anti-human CD8 (clone RPA-T8, Biolegend), anti-human CD45RA (clone HI100, BD Biosciences), anti-human CCR7 (clone G043H7, Biolegend), anti-human CD69 (clone FN50, Biolegend), anti-human HLA-DR (clone L243, Biolegend), anti-human BCL-2 (clone 100, Biolegend), p24 antibodies (anti-HIV core antigen: clone KC57, Beckman Coulter; p24.2 clone 28B7 MediMabs).

Peptide-pulse CTL killing assay

$CD4^+$ T-cells were enriched from PBMCs by magnetic negative selection, following the manufacturer's instructions (StemCell Technologies). Where indicated, these cells were activated prior to peptide pulsing with 1μg/ml each anti-CD3 and anti-CD28 in RPMI-10 media supplemented with 50U/mL of IL-2 (R10-50). Purified $CD4^+$ T-cells were then pulsed with RR11 peptide (RLRDLLLIVTR) (Genscript) at the indicated concentrations for 30 minutes in R10-50. $CD4^+$ T-cells were then washed and co-cultured with autologous, RR11-specific CTL clones in R10-50. After 16 hours, cell cultures were stained with anti-human CD3, CD4, CD8 antibodies, viability dye. In some experiments, cells were also stained with CD45RA and CCR7 antibodies. Cells were then treated with Fixation/Permeabilization solution (BD Biosciences), and followed with BCL-2 intracellularly staining. Samples were analyzed by flow cytometry, and data analysis was performed with FlowJo v10 software (FlowJo, LLC).

RNA-seq sample acquisition

Cultured T_{CM} $CD4^+$ T-cells were generated as previously described (48), see also Supplementary Methods. These T_{CM} $CD4^+$ T-cells were divided into either a "real" or "mock" condition, and then sub-divided into two populations each, receiving either CFSE or cell-track far-red (CTFR) labeling (ThermoFisher Scientific). After staining, $CFSE^+$ cells in the "real" condition were pulsed with 1μg/mL of RR11 peptide for 30 minutes. Following extensive washing, peptide-pulsed cells were mixed with equal numbers of

unpulsed CTFR^{+} cells and co-cultured with CTL clones at an effector:target ratio = 1:1 overnight in R10-50 media. Cells from the "mock" condition did not receive peptide, but were otherwise treated identically to the "real" condition. Following the overnight culture, cells were stained with antibodies against human-CD3, CD4, CD8, and DAPI, and then sorted by FACS Influx (BD Biosciences) directly into vessels containing lysis buffer (Qiagen). Total RNA was immediately extracted using the RNeasy Micro Kit (Qiagen), and RNA quality and concentration was determined by Agilent Bioanalyzer 2100. Library preparation was using the methods of TruSeq RNA Sample Preparation (Non-Stranded and Poly-A selection), and sequencing was run on HiSeq4000 (Illumina) with a single read clustering and 50 cycles of sequencing.

RNA-seq data analysis

The raw sequencing reads in BCL format were processed through bcl2fastq 2.19 (Illumina) for FASTQ conversion and demultiplexing. RNA reads were aligned and mapped to the GRCh37 human reference genome by STAR (Version2.5.2) (https://github.com/alexdobin/STAR) (75), and transcriptome reconstruction was performed by Cufflinks (Version 2.1.1) (http://cole-trapnell-lab.github.io/cufflinks/). The abundance of transcripts was measured with Cufflinks in Fragments Per Kilobase of exon model per Million mapped reads (FPKM) (76, 77). Gene expression profiles were constructed for differential expression, cluster, and principle component analyses with the DESeq2 package (https://bioconductor.org/packages/release/bioc/html/DESeq2.html) (78). For differential expression analysis, pairwise comparisons between two or more groups using parametric tests where read-counts follow a negative binomial distribution with a gene-specific dispersion parameter. Corrected p-values were calculated based on the Benjamini-Hochberg (B-H) method to adjusted for multiple testing. Differential expression genes (DEGs) list between 'real' survivors and 'real' bystanders were determined with a cut-off of FDR (adjusted p-value) <0.05, and then analyzed with ingenuity pathway analysis (IPA, QIAGEN). Significantly enriched pathways were selected with a threshold of B-H multiple testing correction p-value <0.05, and displayed as -log(B-H p-value) >1.3. Molecules interacting networks were also analyzed using

IPA, with the top 25 significantly enriched networks showed in **Table S1**. RNAseq data have been deposited in the GEO repository under the accession number GSE143879.

HIV Flow – Direct staining of HIV-infected cells in ex vivo CD4$^+$ T-cells.

Staining of HIV-infected cells was performed as previously described (44). Briefly, CD4$^+$ T-cells were activated with PMA (25nM) and ionomycin (1μg/mL) for 24 hours at 37^{o}C in R-10 media, and then harvested for flow cytometry. For each sample, around 4-8 x 10^6 cells were stained with viability, anti-human CD3, CD4, CD8, and two intracellular antibodies targeting HIV core antigen, and BCL-2, and then analyzed by flow cytometry (Attune NxT, ThermoFisher Scientific).

Sorting for BCL-2 -> ddPCR

5-10 x 10^6 resting CD4$^+$ T-cells were enriched from long-term ARV-treated participants PBMCs by negative selection. Cells were used for flow cytometry staining with surface antibodies for 30mins 4°C: viability dye and antibodies anti-human CD3, CD4, CD8, with (**Fig. 4B-C**) or without (**Fig. 4A**) CD45RA and CCR7. After washing out the extra surface antibodies, cells were fixed with Biolegend Fixation Buffer for 5mins in 4°C and then permeabilized with Biolegend Permeabilization Wash Buffer and stained intracellularly with anti-human BCL-2 for 30mins. Finally, cells were resuspended in MACS buffer and analyzed/ sorted by flow cytometry (SONY MA9000) based on BCL-2 high vs low. Sorted cells were pelleted and DNA was extracted with QIAamp DNA FFPE minElute kit (Qiagen) following the manufacture protocol. DNA was used for IPDA assays.

HIV Eradication (HIVE) Assays

HIVE assays were set up as previously described (21). Briefly, >20 x 10^6 CD4$^+$ T-cells were pulsed with bryostatin-1 or anti-CD3/anti-CD28 antibodies for 2 hours, then washed and co-cultured with/without ABT-199 and/or HIV-spec. effectors (as indicated in the figures) in HIVE media: XVIVO-15 medium

(Lonza) supplemented with 1μM Tenofovir Disoproxil Fumarate, 1μM nevirapine, 1μM emtricitabine, 10μM T-20, 10U/ml human DNAse I (ProSpec), and 0.1nM IL-7. Following a 3-4 day co-culture, $CD4^+$ T-cells were isolated and rested for 24 hours in R10-50 media at 37°C to allow for ARV washout. Aliquots of pre- and post- CD4 enrichment samples were collected and stained for viability and memory phenotype/activation status with antibodies against anti-human CD3, CD4, CD8, CD45RA, CCR7, CD69 and HLA-DR then analyzed by flow cytometry. Following the overnight culture, a small aliquot of cells was mixed with CountBright™ absolute counting beads and viability dye (Invitrogen Technologies) to obtain a count of total, live $CD4^+$ T-cells by flow cytometry. This viable cell count was used to determine cell numbers for ddPCR and QVOA plating strategies.

Digital droplet PCR

ddPCR measuring total HIV DNA (HIVEs) was performed as previously described (79), with slight modifications. For each PCR reaction, 5 units of restriction enzyme BsaJI (NEB) was directly mixed with 300ng of DNA, ddPCR Supermix (no dUTP) for Probes (Bio-Rad), and final concentrations of 900nM primers and 250nM probe. Primers/Probes were: RPP30 – Fprimer GATTTGGACCTGCGAGCG, Rprimer GCGGCTGTCTCCACAAGT, probe VIC-CTGAACTGAAGGCTCT-MGBNFQ; HIV-gag – Fprimer TCTCGACGCAGGACTCG, Rprimer TACTGACGCTCTCGCACC, probe FAM-CTCTCTCCTTCTAGCCTC-MGBNFQ; Droplets were prepared using the QX200 Droplet Generator (Bio-Rad) following the manufacturer's instructions. Sealed plates were cycled using the following program: 95°C for 10 min; 40 cycles of 94°C for 30 s, 60°C for 1 min; and 98°C for 10 min. Reactions were analyzed using the QX200 Droplet Reader and number of template molecule per μl of starting material was estimated using the Quantalife ddPCR software. 8 technical replicates were run per sample, and we consistently applied a pre-determined exclusion criterion to outliers that deviated from mean values by >2x the standard deviation.

For BCL-2 sorted samples (**Fig. 4**) and HIVEs showing in **Fig. 6**, a modified IPDA(45) was applied. For each PCR reaction, same ddPCR supermix and final concentrations of primers and probes as above, but with 5 units of restriction enzyme Xho I (NEB) mixed with 750ng DNA (HIVEs) or ~250ng DNA (BCL-2 sorted samples, low DNA yield after intracellular staining and flow sorting). Primers and probes were used in 2 separate PCR systems: house-keeping multiplex with RPP30 (same as above) and RPP30-shearing – Fprimer CCATTTGCTGCTCCTTGGG, Rprimer CATGCAAAGGAGGAAGCCG, probe FAM-GGAAAGGAGCAAGGTTC-IABkFQ. HIV multiplex with *gag* primers/probe same as above (HIVEs) or HIV-Ψ (BCL-2 sorted samples) Fprimer- CAGGACTCGGCTTGCTGAAG, Rprimer-GCACCCATCTCTCTCCTTCTAGC, Ψ Probe- FAM-TTTTGGCGTACTCACCAGT-3IABKFQ; and HIV-*env* (RRE) – Fprimer AGTGGTGCAGAGAGAAAAAAGAGC, Rprimer GTCTGGCCTGTACCGTCAGC, probe HEX- CCTTGGGTTCTTGGGA-IABkFQ, hypermutant probe IABkFQ-CCTTAGGTTCTTAGGAGC-IABkFQ (OM5011, OM5148, OM5267, WWH-B008 and WWH-B012). As some samples (OM5334 and WWH-B011) showed low amplification efficiency on *env* signal, we used alternative primers/probe instead. Alt-*env* (RRE) Fprimer ACTATGGGCGCAGCGTC, Rprimer CCCCAGACTGTGAGTTGCA, Probe HEX-CTGGCCTGTACCGTCAG-3IABKFQ. PCR program is as following: 95°C for 10 min; 40 cycles of 94°C for 30 s, 53°C for 1 min; and 98°C for 10 min. DNA input of house-keeping multiplex, is 100-fold (HIVEs) or 30-fold (BCL-2 sorted samples) diluted from the input of HIV-multiplex. Total *gag, env* or 'intact' proviruses copies were calculated by multiplying the dilution factors, and 'Intact provirus' copies were corrected with the shearing percentage calculated from house-keeping multiplex. For HIVEs, 8 technical replicates were run per sample, and applied with a pre-determined exclusion criterion to outliers that deviated from mean values by >2x the standard deviation. For BCL-2 sorted samples, 4-6 technical replicates were run per sample, and merged data from QuantaSoft software was exported and analyzed.

Quantitative viral outgrowth assays (QVOAs)

588 QVOAs were performed using a previously described protocol (80), with slight modifications depending
589 on the application. Live cells counted by flow cytometry were distributed into either three of 2-fold serial
590 dilutions with 8 or 12 replicates per dilution, or four of 2-fold serial dilutions with 24 replicates per dilution.
591 This was determined based on the numbers of viable cells recovered at the end of each HIVE assay and the
592 baseline IUPM values of the donor. At least $3x10^6$ cells were plated for any given QVOA (where cell
593 numbers fell below this threshold, QVOA assays were omitted). Cells were then stimulated with 2µg/ml of
594 PHA (ThermoFisher Scientific) + 10^6 PBMCs (HIV^- donor, irradiated at 5000 rads). The next day, 10^6
595 $CCR5^+$MOLT-4 cells were added along with a half media change. Cultures were then incubated for 14 days,
596 with half media changes with R10-50 every 3-4 days. We performed p24 ELISA on supernatant 15d after
597 the PHA stimulation. For each condition, values for cells/well, number of positive wells, and total wells
598 tested were entered into a limiting dilution analyzer (http://bioinf.wehi.edu.au/software/elda/) to calculate
599 the maximal likelihood IUPM and a corresponding 95% confidence interval.
600
601 *Quantification and Statistical Analysis*
602 Statistical analyses were performed using Prism 7 (GraphPad), and the statistical analysis methods used are
603 reported in Figure Legends. Comparisons among different peptide concentrations used Student's t-test (2-
604 tailed). Comparisons between BCL-2 MFI of Gag^+ vs Gag^- population in HIV-Flow used unpaired non-
605 parametric test (2-tailed) - Wilcoxon signed rank test. Comparisons between BCL-2^{hi} vs BCL-2^{low} sorted
606 samples used paired non-parametric test (2-tailed) - Wilcoxon matched-pairs signed rank test. All ddPCR
607 data were analyzed by Ordinary one-way ANOVA, with Tukey's multiple comparisons test if ANOVA test
608 was significant, and statistics for the summary data sets for HIV DNA were performed using the mean of 8
609 replicates per condition. QVOAs were run at the end of each HIVE assay, and the IUPM was calculated as
610 described above, and Chi-square test was applied to determine the significance. All comparisons between
611 HIVE conditions used paired non-parametric test (2-tailed) - Wilcoxon matched-pairs signed rank test. A
612 P value of less than 0.05 was considered significant.
613

Study Approval

HIV-positive individuals were recruited from either the Maple Leaf Medical Clinic in Toronto, Canada through a protocol approved by the University of Toronto Institutional Review Board (IRB), or Whitman-Walker Health in Washington D.C. (**Table 1**). Some samples were also collected through an IRB approved protocol at the Rockefeller University (New York) (**Table 2**). Additional use of de-identified samples was reviewed and approved by the George Washington University (Washington, D.C.), and Weill Cornell Medicine (New York) Institutional Review Boards. All subjects were adults, and gave written informed consent prior to their participation. Leukapheresis samples were used immediately if possible, or cryopreserved in liquid nitrogen; cells were not left in culture prior to the initiation of experiments.

Author contributions: RBJ, YR, and SHH conceptualized the study. RBJ, YR, SHH, SP, WCA, DM, DA, ABM, AB, CMB developed the methodology. RBJ, YR, SHH, SP, WCA, DM, DA, ABM, RD, DC, EZ, TM, RT, TR, CDM conducted the investigation. CMK, EB, AW, CC, WDH provided resources in the form of clinical samples. RBJ, YR, and SHH analyzed data and wrote the manuscript, reviewed by all authors. RBJ, AB, and CMB acquired funding. RBJ supervised the study. YR and SHH share first authorship. Authorship order for the 2 co-first authors was determined based on their time of entry into the project (YR entered the project before SHH).

Acknowledgments

We thank Marina Caskey for providing de-identified samples from ART-naïve donors used in this study. We also thank Natalie Kinloch and Zabrina Brumme for designing the alternative ddPCR primers. This work was supported by the NIH funded R01grants AI31798 and AI147845. It was also supported in part

639 by the Martin Delaney 'BELIEVE' Collaboratory (NIH grant 1UM1AI26617); and the NIH funded Center
640 for AIDS Research grants (P30 AI117970), which are both supported by the following NIH Co-Funding
641 and Participating Institutes and Centers: NIAID, NCI, NICHD, NHLBI, NIDA, NIMH, NIA, FIC, and OAR.
642 The following reagents were obtained from the NIH AIDS Research and Reference Reagent Program: IL-
643 2, pNL4-3, $CCR5^+$ MOLT-4 cells. Reagents for HIV p24 ELISAs were obtained from the NCI's AIDS and
644 Cancer Virus Program.
645

References

1. Turk G, Ghiglione Y, Falivene J, Socias ME, Laufer N, Coloccini RS, et al. Early Gag immunodominance of the HIV-specific T-cell response during acute/early infection is associated with higher CD8+ T-cell antiviral activity and correlates with preservation of the CD4+ T-cell compartment. *J Virol.* 2013;87(13):7445-62.
2. Turnbull EL, Lopes AR, Jones NA, Cornforth D, Newton P, Aldam D, et al. HIV-1 epitope-specific CD8+ T cell responses strongly associated with delayed disease progression cross-recognize epitope variants efficiently. *J Immunol.* 2006;176(10):6130-46.
3. Betts MR, Nason MC, West SM, De Rosa SC, Migueles SA, Abraham J, et al. HIV nonprogressors preferentially maintain highly functional HIV-specific CD8+ T cells. *Blood.* 2006;107(12):4781-9.
4. Altfeld M, Kalife ET, Qi Y, Streeck H, Lichterfeld M, Johnston MN, et al. HLA Alleles Associated with Delayed Progression to AIDS Contribute Strongly to the Initial CD8(+) T Cell Response against HIV-1. *PLoS Med.* 2006;3(10):e403.
5. Day CL, Kiepiela P, Leslie AJ, van der Stok M, Nair K, Ismail N, et al. Proliferative capacity of epitope-specific CD8 T-cell responses is inversely related to viral load in chronic human immunodeficiency virus type 1 infection. *J Virol.* 2007;81(1):434-8.
6. Cartwright EK, Spicer L, Smith SA, Lee D, Fast R, Paganini S, et al. CD8(+) Lymphocytes Are Required for Maintaining Viral Suppression in SIV-Infected Macaques Treated with Short-Term Antiretroviral Therapy. *Immunity.* 2016;45(3):656-68.
7. Jones RB, and Walker BD. HIV-specific CD8(+) T cells and HIV eradication. *The Journal of clinical investigation.* 2016;126(2):455-63.
8. Yang OO, Kalams SA, Trocha A, Cao H, Luster A, Johnson RP, et al. Suppression of human immunodeficiency virus type 1 replication by CD8+ cells: evidence for HLA class I-restricted triggering of cytolytic and noncytolytic mechanisms. *Journal of virology.* 1997;71(4):3120-8.
9. Migueles SA, Osborne CM, Royce C, Compton AA, Joshi RP, Weeks KA, et al. Lytic granule loading of CD8+ T cells is required for HIV-infected cell elimination associated with immune control. *Immunity.* 2008;29(6):1009-21.
10. Chun TW, Finzi D, Margolick J, Chadwick K, Schwartz D, and Siliciano RF. In vivo fate of HIV-1-infected T cells: quantitative analysis of the transition to stable latency. *Nature medicine.* 1995;1(12):1284-90.
11. Finzi D, Hermankova M, Pierson T, Carruth LM, Buck C, Chaisson RE, et al. Identification of a reservoir for HIV-1 in patients on highly active antiretroviral therapy. *Science.* 1997;278(5341):1295-300.
12. Wong JK, Hezareh M, Gunthard HF, Havlir DV, Ignacio CC, Spina CA, et al. Recovery of replication-competent HIV despite prolonged suppression of plasma viremia. *Science.* 1997;278(5341):1291-5.
13. Shan L, Deng K, Shroff NS, Durand CM, Rabi SA, Yang HC, et al. Stimulation of HIV-1-specific cytolytic T lymphocytes facilitates elimination of latent viral reservoir after virus reactivation. *Immunity.* 2012;36(3):491-501.
14. Deeks SG. HIV: Shock and kill. *Nature.* 2012;487(7408):439-40.
15. Sogaard OS, Graversen ME, Leth S, Olesen R, Brinkmann CR, Nissen SK, et al. The Depsipeptide Romidepsin Reverses HIV-1 Latency In Vivo. *PLoS pathogens.* 2015;11(9):e1005142.
16. Rasmussen TA, Tolstrup M, Moller HJ, Brinkmann CR, Olesen R, Erikstrup C, et al. Activation of latent human immunodeficiency virus by the histone deacetylase inhibitor panobinostat: a pilot study to assess effects on the central nervous system. *Open Forum Infect Dis.* 2015;2(1):ofv037.
17. Rasmussen TA, Tolstrup M, Brinkmann CR, Olesen R, Erikstrup C, Solomon A, et al. Panobinostat, a histone deacetylase inhibitor, for latent-virus reactivation in HIV-infected patients on suppressive antiretroviral therapy: a phase 1/2, single group, clinical trial. *Lancet HIV.* 2014;1(1):e13-21.
18. Ke R, Lewin SR, Elliott JH, and Perelson AS. Modeling the Effects of Vorinostat In Vivo Reveals both Transient and Delayed HIV Transcriptional Activation and Minimal Killing of Latently Infected Cells. *PLoS Pathog.* 2015;11(10):e1005237.
19. van Praag RM, Prins JM, Roos MT, Schellekens PT, Ten Berge IJ, Yong SL, et al. OKT3 and IL-2 treatment for purging of the latent HIV-1 reservoir in vivo results in selective long-lasting CD4+ T cell depletion. *J Clin Immunol.* 2001;21(3):218-26.

20. Dybul M, Hidalgo B, Chun TW, Belson M, Migueles SA, Justement JS, et al. Pilot study of the effects of intermittent interleukin-2 on human immunodeficiency virus (HIV)-specific immune responses in patients treated during recently acquired HIV infection. *J Infect Dis.* 2002;185(1):61-8.
21. Huang SH, Ren Y, Thomas AS, Chan D, Mueller S, Ward AR, et al. Latent HIV reservoirs exhibit inherent resistance to elimination by CD8+ T cells. *J Clin Invest.* 2018;128(2):876-89.
22. Huang S-H, McCann, C.D., Mota, T.M., Wang, C., Lipkin, S.M., Jones, R. B. Have Cells Harboring the HIV Reservoir Been Immunoedited? *Frontiers in immunology.* 2019;10.
23. Veenhuis RT, Kwaa AK, Garliss CC, Latanich R, Salgado M, Pohlmeyer CW, et al. Long-term remission despite clonal expansion of replication-competent HIV-1 isolates. *JCI Insight.* 2018;3(18).
24. Liu J, and Roederer M. Differential susceptibility of leukocyte subsets to cytotoxic T cell killing: implications for HIV immunopathogenesis. *Cytometry A.* 2007;71(2):94-104.
25. Buzon MJ, Yang Y, Ouyang Z, Sun H, Seiss K, Rogich J, et al. Susceptibility to CD8 T-cell-mediated killing influences the reservoir of latently HIV-1-infected CD4 T cells. *J Acquir Immune Defic Syndr.* 2014;65(1):1-9.
26. Balaji KN, Schaschke N, Machleidt W, Catalfamo M, and Henkart PA. Surface cathepsin B protects cytotoxic lymphocytes from self-destruction after degranulation. *J Exp Med.* 2002;196(4):493-503.
27. Cohnen A, Chiang SC, Stojanovic A, Schmidt H, Claus M, Saftig P, et al. Surface CD107a/LAMP-1 protects natural killer cells from degranulation-associated damage. *Blood.* 2013;122(8):1411-8.
28. Clayton KL, Collins DR, Lengieza J, Ghebremichael M, Dotiwala F, Lieberman J, et al. Resistance of HIV-infected macrophages to CD8(+) T lymphocyte-mediated killing drives activation of the immune system. *Nat Immunol.* 2018;19(5):475-86.
29. Medema JP, de Jong J, Peltenburg LT, Verdegaal EM, Gorter A, Bres SA, et al. Blockade of the granzyme B/perforin pathway through overexpression of the serine protease inhibitor PI-9/SPI-6 constitutes a mechanism for immune escape by tumors. *Proc Natl Acad Sci U S A.* 2001;98(20):11515-20.
30. Halle S, Halle O, and Forster R. Mechanisms and Dynamics of T Cell-Mediated Cytotoxicity In Vivo. *Trends Immunol.* 2017;38(6):432-43.
31. Nagata S. Fas ligand-induced apoptosis. *Annu Rev Genet.* 1999;33:29-55.
32. Nagata S, and Golstein P. The Fas death factor. *Science.* 1995;267(5203):1449-56.
33. Youle RJ, and Strasser A. The BCL-2 protein family: opposing activities that mediate cell death. *Nat Rev Mol Cell Biol.* 2008;9(1):47-59.
34. Adams JM, and Cory S. The Bcl-2 protein family: arbiters of cell survival. *Science.* 1998;281(5381):1322-6.
35. Hanahan D, and Weinberg RA. The hallmarks of cancer. *Cell.* 2000;100(1):57-70.
36. Charo J, Finkelstein SE, Grewal N, Restifo NP, Robbins PF, and Rosenberg SA. Bcl-2 overexpression enhances tumor-specific T-cell survival. *Cancer research.* 2005;65(5):2001-8.
37. Pawlowski J, and Kraft AS. Bax-induced apoptotic cell death. *Proceedings of the National Academy of Sciences of the United States of America.* 2000;97(2):529-31.
38. Garcia-Aranda M, Perez-Ruiz E, and Redondo M. Bcl-2 Inhibition to Overcome Resistance to Chemo- and Immunotherapy. *International journal of molecular sciences.* 2018;19(12).
39. Souers AJ, Leverson JD, Boghaert ER, Ackler SL, Catron ND, Chen J, et al. ABT-199, a potent and selective BCL-2 inhibitor, achieves antitumor activity while sparing platelets. *Nat Med.* 2013;19(2):202-8.
40. Roberts AW, Seymour JF, Brown JR, Wierda WG, Kipps TJ, Khaw SL, et al. Substantial susceptibility of chronic lymphocytic leukemia to BCL2 inhibition: results of a phase I study of navitoclax in patients with relapsed or refractory disease. *J Clin Oncol.* 2012;30(5):488-96.
41. Chomont N, El-Far M, Ancuta P, Trautmann L, Procopio FA, Yassine-Diab B, et al. HIV reservoir size and persistence are driven by T cell survival and homeostatic proliferation. *Nature medicine.* 2009;15(8):893-900.
42. Sallusto F, Lenig D, Forster R, Lipp M, and Lanzavecchia A. Two subsets of memory T lymphocytes with distinct homing potentials and effector functions. *Nature.* 1999;401(6754):708-12.
43. Bosque A, and Planelles V. Studies of HIV-1 latency in an ex vivo model that uses primary central memory T cells. *Methods.* 2011;53(1):54-61.
44. Pardons M, Baxter AE, Massanella M, Pagliuzza A, Fromentin R, Dufour C, et al. Single-cell characterization and quantification of translation-competent viral reservoirs in treated and untreated HIV infection. *PLoS pathogens.* 2019;15(2):e1007619.
45. Bruner KM, Wang Z, Simonetti FR, Bender AM, Kwon KJ, Sengupta S, et al. A quantitative approach for measuring the reservoir of latent HIV-1 proviruses. *Nature.* 2019;566(7742):120-5.

46. Cummins NW, Sainski AM, Dai H, Natesampillai S, Pang YP, Bren GD, et al. Prime, Shock, and Kill: Priming CD4 T Cells from HIV Patients with a BCL-2 Antagonist before HIV Reactivation Reduces HIV Reservoir Size. *J Virol.* 2016;90(8):4032-48.
47. Ho YC, Shan L, Hosmane NN, Wang J, Laskey SB, Rosenbloom DI, et al. Replication-competent noninduced proviruses in the latent reservoir increase barrier to HIV-1 cure. *Cell.* 2013;155(3):540-51.
48. Bosque A, and Planelles V. Induction of HIV-1 latency and reactivation in primary memory CD4+ T cells. *Blood.* 2009;113(1):58-65.
49. Martins LJ, Bonczkowski P, Spivak AM, De Spiegelaere W, Novis CL, DePaula-Silva AB, et al. Modeling HIV-1 Latency in Primary T Cells Using a Replication-Competent Virus. *AIDS Res Hum Retroviruses.* 2016;32(2):187-93.
50. Lam S, Sung J, Cruz C, Castillo-Caro P, Ngo M, Garrido C, et al. Broadly-specific cytotoxic T cells targeting multiple HIV antigens are expanded from HIV+ patients: implications for immunotherapy. *Mol Ther.* 2015;23(2):387-95.
51. Patel S, Lam S, Cruz CR, Wright K, Cochran C, Ambinder RF, et al. Functionally Active HIV-Specific T Cells that Target Gag and Nef Can Be Expanded from Virus-Naive Donors and Target a Range of Viral Epitopes: Implications for a Cure Strategy after Allogeneic Hematopoietic Stem Cell Transplantation. *Biol Blood Marrow Transplant.* 2016;22(3):536-41.
52. Day CL, Kaufmann DE, Kiepiela P, Brown JA, Moodley ES, Reddy S, et al. PD-1 expression on HIV-specific T cells is associated with T-cell exhaustion and disease progression. *Nature.* 2006;443(7109):350-4.
53. Jones RB, Ndhlovu LC, Barbour JD, Sheth PM, Jha AR, Long BR, et al. Tim-3 expression defines a novel population of dysfunctional T cells with highly elevated frequencies in progressive HIV-1 infection. *J Exp Med.* 2008;205(12):2763-79.
54. Petrovas C, Casazza JP, Brenchley JM, Price DA, Gostick E, Adams WC, et al. PD-1 is a regulator of virus-specific CD8+ T cell survival in HIV infection. *J Exp Med.* 2006;203(10):2281-92.
55. Trautmann L, Janbazian L, Chomont N, Said EA, Gimmig S, Bessette B, et al. Upregulation of PD-1 expression on HIV-specific CD8+ T cells leads to reversible immune dysfunction. *Nat Med.* 2006;12(10):1198-202.
56. Hersperger AR, Migueles SA, Betts MR, and Connors M. Qualitative features of the HIV-specific CD8+ T-cell response associated with immunologic control. *Curr Opin HIV AIDS.* 2011;6(3):169-73.
57. Zaretsky JM, Garcia-Diaz A, Shin DS, Escuin-Ordinas H, Hugo W, Hu-Lieskovan S, et al. Mutations Associated with Acquired Resistance to PD-1 Blockade in Melanoma. *The New England journal of medicine.* 2016;375(9):819-29.
58. Patel SJ, Sanjana NE, Kishton RJ, Eidizadeh A, Vodnala SK, Cam M, et al. Identification of essential genes for cancer immunotherapy. *Nature.* 2017;548(7669):537-42.
59. Letai AG. Diagnosing and exploiting cancer's addiction to blocks in apoptosis. *Nat Rev Cancer.* 2008;8(2):121-32.
60. Deng J, Carlson N, Takeyama K, Dal Cin P, Shipp M, and Letai A. BH3 profiling identifies three distinct classes of apoptotic blocks to predict response to ABT-737 and conventional chemotherapeutic agents. *Cancer Cell.* 2007;12(2):171-85.
61. Del Gaizo Moore V, Brown JR, Certo M, Love TM, Novina CD, and Letai A. Chronic lymphocytic leukemia requires BCL2 to sequester prodeath BIM, explaining sensitivity to BCL2 antagonist ABT-737. *J Clin Invest.* 2007;117(1):112-21.
62. Ito T, Deng X, Carr B, and May WS. Bcl-2 phosphorylation required for anti-apoptosis function. *The Journal of biological chemistry.* 1997;272(18):11671-3.
63. Natesampillai S, Cummins NW, Nie Z, Sampath R, Baker JV, Henry K, et al. HIV Protease-Generated Casp8p41, When Bound and Inactivated by Bcl2, Is Degraded by the Proteasome. *J Virol.* 2018;92(13).
64. Cummins NW, Sainski-Nguyen AM, Natesampillai S, Aboulnasr F, Kaufmann S, and Badley AD. Maintenance of the HIV Reservoir Is Antagonized by Selective BCL2 Inhibition. *J Virol.* 2017;91(11).
65. Archin NM, and Margolis DM. Emerging strategies to deplete the HIV reservoir. *Current opinion in infectious diseases.* 2014;27(1):29-35.
66. Perelson AS, Neumann AU, Markowitz M, Leonard JM, and Ho DD. HIV-1 dynamics in vivo: virion clearance rate, infected cell life-span, and viral generation time. *Science.* 1996;271(5255):1582-6.
67. Wang Z, Gurule EE, Brennan TP, Gerold JM, Kwon KJ, Hosmane NN, et al. Expanded cellular clones carrying replication-competent HIV-1 persist, wax, and wane. *Proc Natl Acad Sci U S A.* 2018;115(11):E2575-E84.

68. Kuo HH, Ahmad R, Lee GQ, Gao C, Chen HR, Ouyang Z, et al. Anti-apoptotic Protein BIRC5 Maintains Survival of HIV-1-Infected CD4(+) T Cells. *Immunity.* 2018;48(6):1183-94 e5.
69. Pollack RA, Jones RB, Pertea M, Bruner KM, Martin AR, Thomas AS, et al. Defective HIV-1 Proviruses Are Expressed and Can Be Recognized by Cytotoxic T Lymphocytes, which Shape the Proviral Landscape. *Cell host & microbe.* 2017;21(4):494-506 e4.
70. Imamichi H, Dewar RL, Adelsberger JW, Rehm CA, O'Doherty U, Paxinos EE, et al. Defective HIV-1 proviruses produce novel protein-coding RNA species in HIV-infected patients on combination antiretroviral therapy. *Proceedings of the National Academy of Sciences of the United States of America.* 2016;113(31):8783-8.
71. Boidol B, Kornauth C, van der Kouwe E, Prutsch N, Kazianka L, Gultekin S, et al. First-in-human response of BCL-2 inhibitor venetoclax in T-cell prolymphocytic leukemia. *Blood.* 2017;130(23):2499-503.
72. Seymour JF, Kipps TJ, Eichhorst B, Hillmen P, D'Rozario J, Assouline S, et al. Venetoclax-Rituximab in Relapsed or Refractory Chronic Lymphocytic Leukemia. *N Engl J Med.* 2018;378(12):1107-20.
73. Mathew R, Haribhai D, Kohlhapp F, Duggan R, Ellis P, Riehm JJ, et al. The BCL-2-Selective Inhibitor Venetoclax Spares Activated T-Cells during Anti-Tumor Immunity. *Blood.* 2018;132(Suppl 1):3704-.
74. Haikala HM, Anttila JM, Marques E, Raatikainen T, Ilander M, Hakanen H, et al. Pharmacological reactivation of MYC-dependent apoptosis induces susceptibility to anti-PD-1 immunotherapy. *Nat Commun.* 2019;10(1):620.
75. Dobin A, Davis CA, Schlesinger F, Drenkow J, Zaleski C, Jha S, et al. STAR: ultrafast universal RNA-seq aligner. *Bioinformatics.* 2013;29(1):15-21.
76. Trapnell C, Hendrickson DG, Sauvageau M, Goff L, Rinn JL, and Pachter L. Differential analysis of gene regulation at transcript resolution with RNA-seq. *Nat Biotechnol.* 2013;31(1):46-53.
77. Trapnell C, Williams BA, Pertea G, Mortazavi A, Kwan G, van Baren MJ, et al. Transcript assembly and quantification by RNA-Seq reveals unannotated transcripts and isoform switching during cell differentiation. *Nat Biotechnol.* 2010;28(5):511-5.
78. Love MI, Huber W, and Anders S. Moderated estimation of fold change and dispersion for RNA-seq data with DESeq2. *Genome Biol.* 2014;15(12):550.
79. Strain MC, Lada SM, Luong T, Rought SE, Gianella S, Terry VH, et al. Highly precise measurement of HIV DNA by droplet digital PCR. *PloS one.* 2013;8(4):e55943.
80. Laird GM, Eisele EE, Rabi SA, Lai J, Chioma S, Blankson JN, et al. Rapid quantification of the latent reservoir for HIV-1 using a viral outgrowth assay. *PLoS pathogens.* 2013;9(5):e1003398.

Figure 1

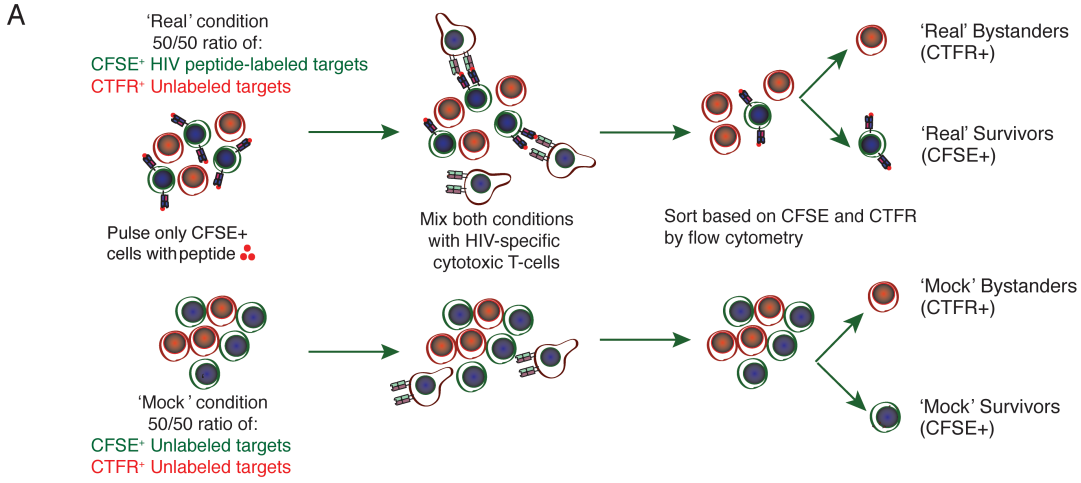

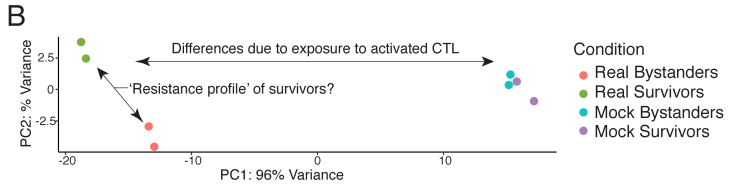

D

GeneName	Count
RALA	8
RALB	7
RAP1A	7
BCL2	5
PPP2R5D	4
RPS27A	4

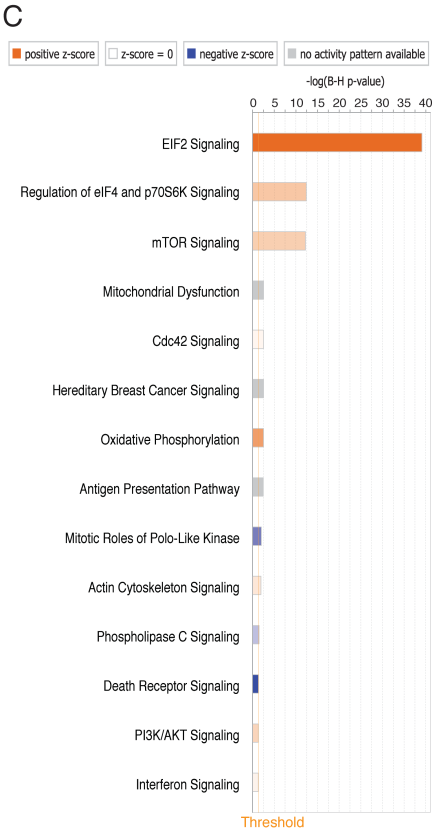

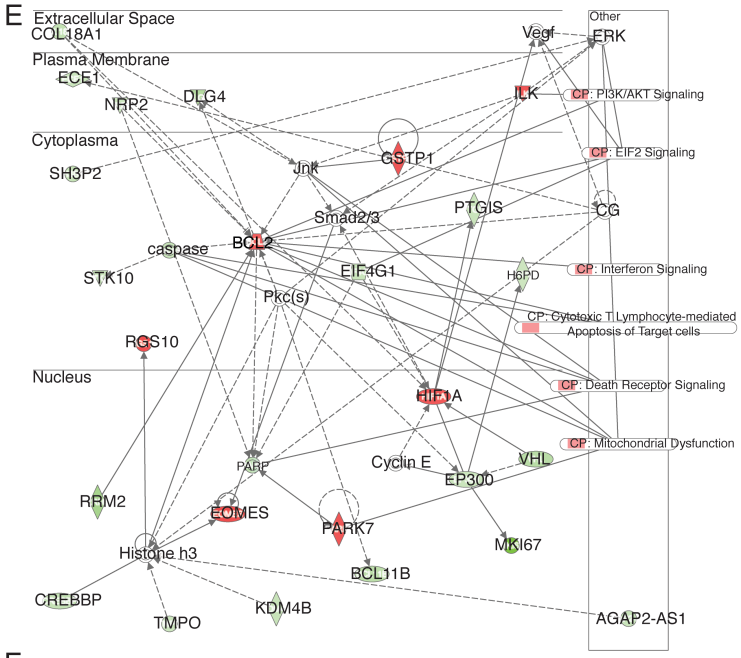

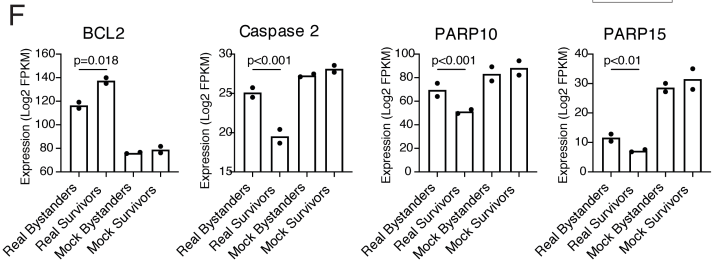

Fig. 1. Transcriptional Profiling of Target CD4$^+$ T-cells that Survive CTL Co-culture Reveals Candidate Mechanisms of Resistance. (A) Schematic of peptide-pulse killing assay and flow sorting for transcriptional profiling. **(B)** Principal component analysis (PCA) showing clustering of cell populations, as indicated. **(C)** Ingenuity pathway analysis results showing the significant enriched pathways between 'real bystanders' and 'real survivors'. Orange bars indicate positive z-scores, blue bars - negative z-score and grey bars – no activity pattern. **(D)** Top 6 genes by numbers of instances in significant pathways from **C**. **(E)** IPA network analysis (subcellular display) showing a significantly enriched network. Interactions with significant pathways from **C** and with cytotoxic T Lymphocyte-mediated Apoptosis of Target Cells are also shown. Red shading indicates over-expressed in 'real survivors', and green indicates under-expressed – both in comparison to 'real bystanders'. **(F)** BCL2 as well as upstream (CASP2) and downstream (PARP) gene expression levels in all 4 conditions. Shown are fragments per kilobase of transcript per million mapped reads (FPKM) from RNA-seq. False discovery rate adj. p-values from DESeq analysis are shown.

Figure 2

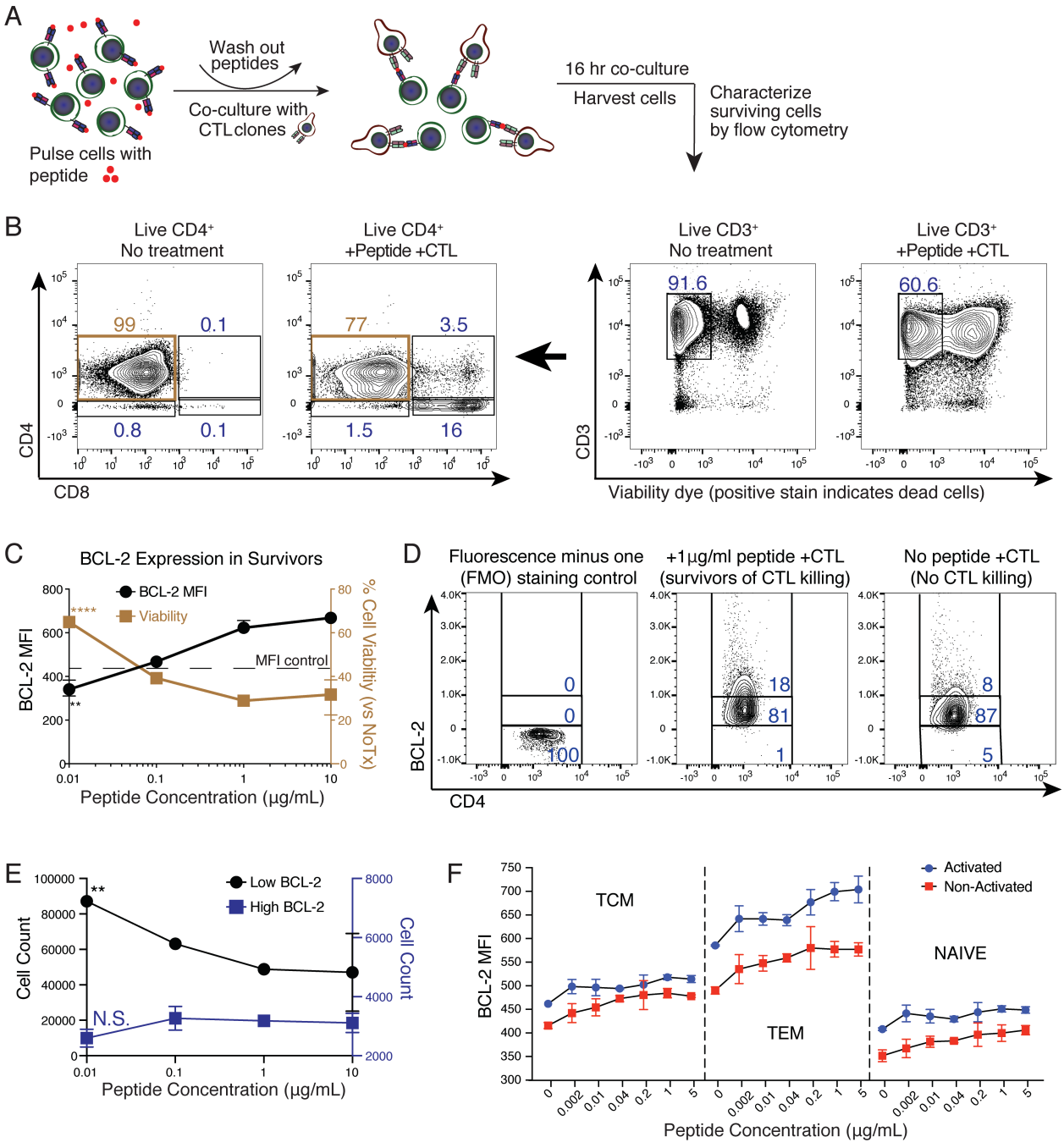

859

860 **Fig. 2. CD8$^+$ CTL preferentially eliminate CD4$^+$ T-cells with low BCL-2 expression levels. (A)**

861 Schematic of peptide-pulse and killing assay. **(B)** Representative gating strategy of flow cytometry plots to

862 identify surviving CD4$^+$ T-cells, and CD4:CD8 ratios in either "No Treatment" or "+Peptide+CTL"

863 conditions. **(C)** Graph of total BCL-2 MFI (left axis, black line) and CD4$^+$ T-cell viability normalized to

the NoTx condition (right axis, brown line), following a peptide-pulse killing assay. Total BCL-2 MFI was calculated based on viable $CD4^+$ T-cells. The dashed line indicates the BCL-2 MFI of an untreated control. **(D)** Flow cytometry plots depicting BCL-2 gating strategy for BCL-2^{hi} and BCL-2^{low} populations. **(E)** Graph depicting $CD4^+$ T-cell counts in BCL-2^{hi} (right axis, blue) and BCL-2^{low} (left axis, black) populations after CTL killing with different concentration peptide-pulsing treatments. Samples were run in triplicates, and shown are median±range. (**F**) The data shown are analogous to panel **C**, but with two additions: i) killing assays were performed in parallel on $CD4^+$ cells that had either been activated with anti-CD3/anti-CD28, or were used directly *ex vivo* (non-activated) ii) the markers CD45RA and CCR7 were included in the flow panel to discriminate naïve ($CD45RA^+CCR7^+$), TCM ($CD45RA^-CCR7^+$), and TEM ($CD45RA^-CCR7^-$). Statistical significance was determined by t-test, * $p<0.05$, ** $p<0.01$, *** $p<0.001$, **** $p<0.0001$

Figure 3

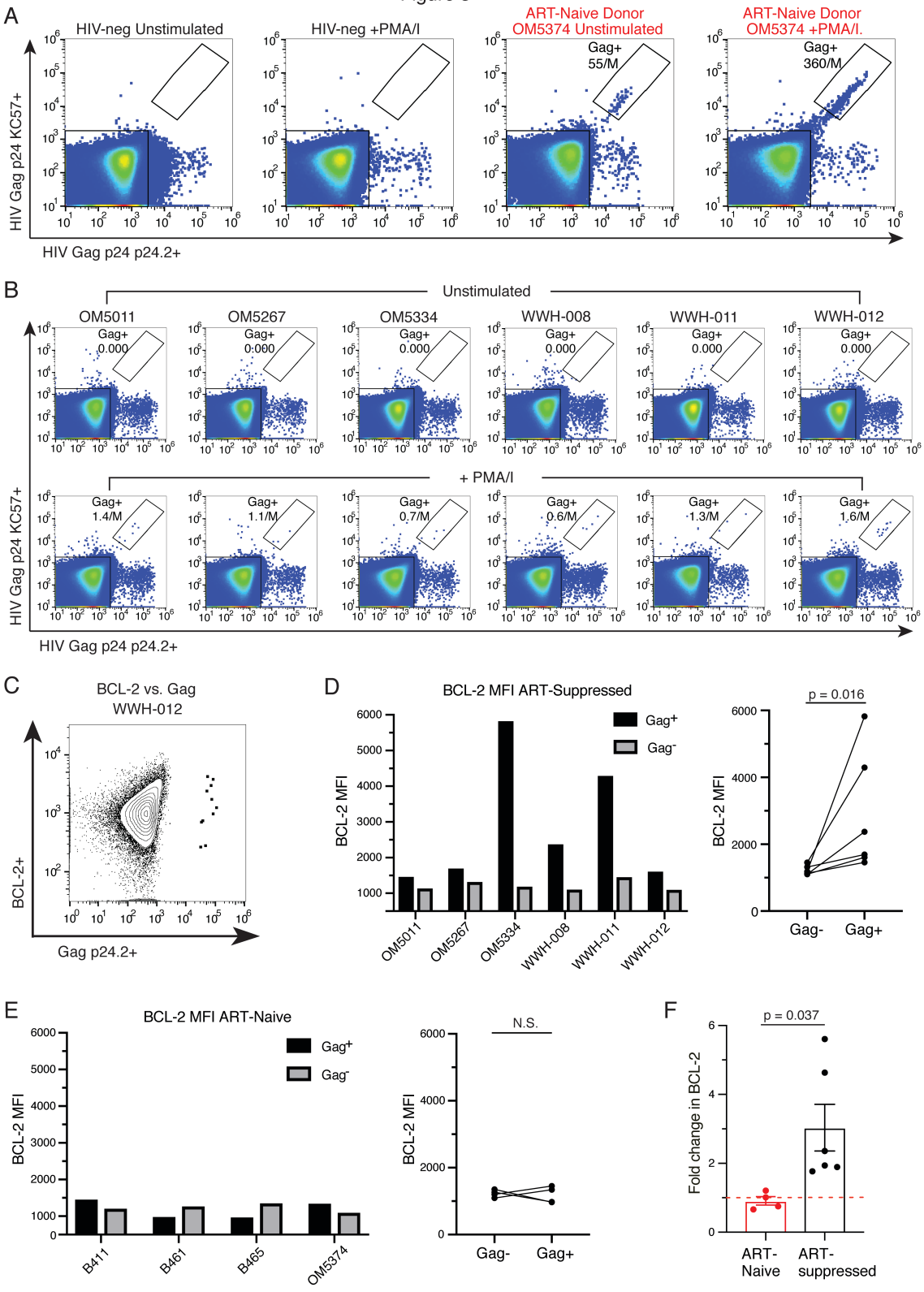
A
HIV-neg Unstimulated
HIV-neg +PMA/I
ART-Naive Donor OM5374 Unstimulated
ART-Naive Donor OM5374 +PMA/I.
Gag+ 55/M
Gag+ 360/M
HIV Gag p24 KC57+
HIV Gag p24 p24.2+
B
Unstimulated
+ PMA/I
OM5011
OM5267
OM5334
WWH-008
WWH-011
WWH-012
Gag+ 0.000
Gag+ 1.4/M
Gag+ 1.1/M
Gag+ 0.7/M
Gag+ 0.6/M
Gag+ 1.3/M
Gag+ 1.6/M
C
BCL-2 vs. Gag
WWH-012
BCL-2+
Gag p24.2+
D
BCL-2 MFI ART-Suppressed
Gag+
Gag-
BCL-2 MFI
p = 0.016
Gag-
Gag+
E
BCL-2 MFI ART-Naive
B411
B461
B465
OM5374
N.S.
F
p = 0.037
Fold change in BCL-2
ART-Naive
ART-suppressed

Fig. 3. HIV reservoirs are preferentially harbored in BCL-2^{high} expressing CD4^{+} T-cells following *ex vivo* reactivation. **(A)** Flow cytometry plots depicting strategy for identifying HIV expressing cells, by gating on populations that were double positive for the two HIV Gag antibodies. Each plot represents 4-8x10^{6} events. **(B)** Flow cytometry plots showing HIV expressing cells from 6 HIV-infected ART-suppressed donors: unstimulated (top row) and stimulated with PMA/I (bottom row). The numbers adjacent to the Gag^{+} gates indicate the numbers of events detected per million cells. **(C)** Flow cytometry plot depicting BCL-2 vs Gag expression in *ex vivo* CD4^{+} T-cells from an ART suppressed donor. **(D&E)** BCL-2 MFI of Gag^{+} and Gag^{-} populations in *ex vivo* CD4^{+} T-cells from **(D)** ART-suppressed donors (the same donors as B) **or (E)** 4 ARV-naive donors, after PMA/I stimulation (Wilcoxon signed rank test). **(F)** Significantly greater differences in BCL-2 expression, between Gag^{+} and Gag^{-} CD4^{+} T-cells, were observed in ART-suppressed donors, compared to ART-naïve individuals (unpaired t-test).

Figure 4

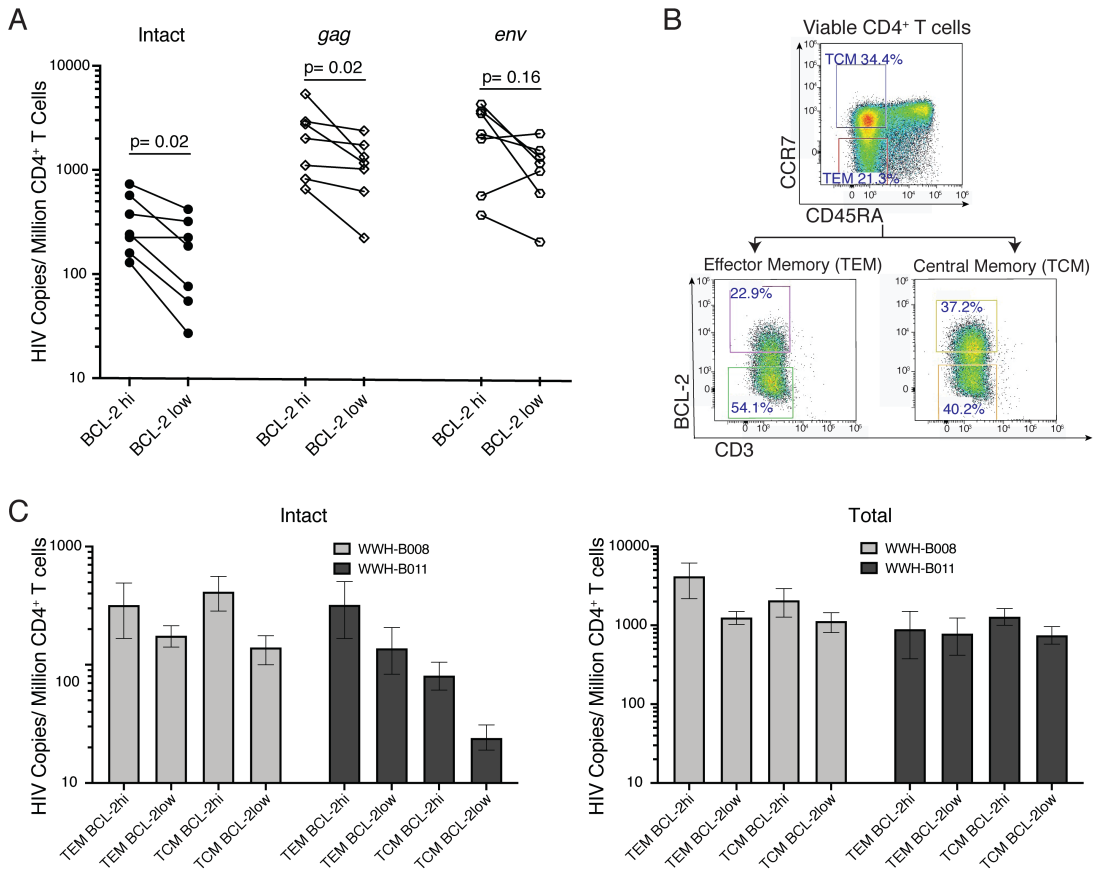

Fig. 4. Intact HIV proviruses are preferentially harbored in BCL-2^{high} expressing CD4^{+} T-cells *ex vivo*. **(A)** Shown are droplet digital PCR (ddPCR) results quantifying HIV DNA in resting *ex vivo* CD4^{+} T-cells from ARV-treated donors that had been flow cytometry sorted based on BCL-2 expression. 'Intact' = quantification based on droplets that were double positive for *gag* and *env* signals (represent full-length proviruses); '*gag*' = quantification based on any droplet that amplified with *gag* primer/probes, '*env*' = quantification based on any droplet that amplified with *env* primer/probes (Wilcoxon matched-pairs signed rank test, n=7). **(B)** Flow cytometry plots depicting sorting based on both memory phenotype and BCL-2 expression, using CD45RA and CCR7 to separate central memory (TCM) and effector memory (TEM) populations. **(C)** 'Intact' and '*gag*'(see **A**, above) ddPCR results on samples from two ARV-treated donors – WWH-B008 (corresponds to flow plots in **B**), and WWH-B011. Note that the difference in presentation and analysis of these ddPCR data versus other ddPCR data in the manuscript is due to the low DNA yield

post BCL-2 intracellular staining and flow sorting. Whereas in other experiments each of 8 ddPCR replicates were treated as individual data-points, here the ddPCR software (Quantasoft) generated maximum likelihood estimates 95% confidence intervals (shown) based on the frequency of positive droplets for all 4-6 replicates taken together. This analysis method is recommended by the instrument manufacturer for the analysis of rare events.

Figure 5

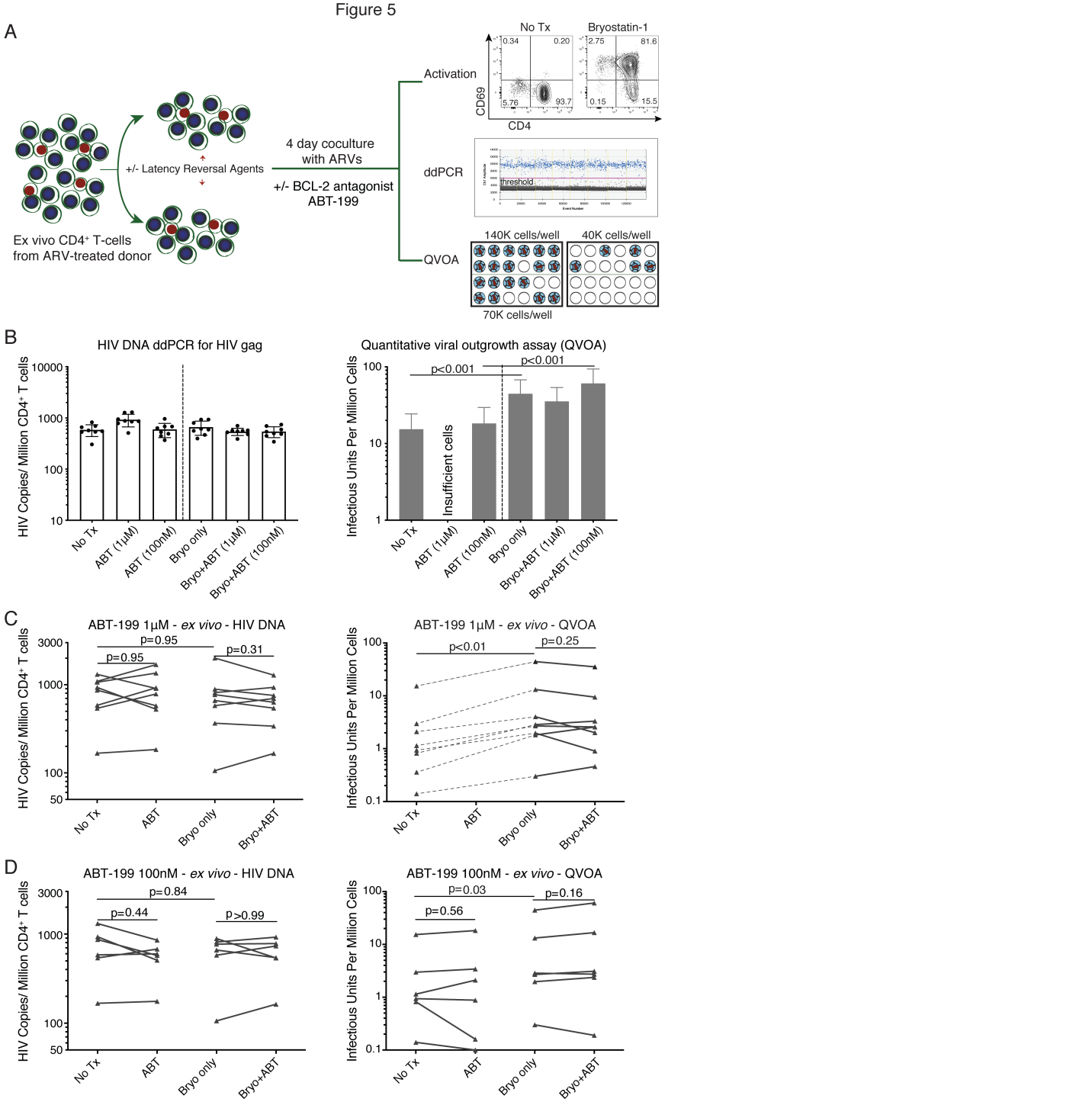

Fig. 5. BCL-2 antagonist ABT-199 failed to drive reductions in *ex vivo*, latently infected CD4$^+$ T-cells in HIVE assays. (A) Schematic of a HIVE assay using *ex vivo* CD4$^+$ T-cells from ART-suppressed individual showing endpoints. **(B)** A representative HIVE assay showing total HIV DNA (left, means ± SD of 8 replicates) and infectious unites per million cells (IUPM, right, ± 95% confidence interval). Statistical

909 significance determined by: One-way ANOVA for ddPCR, and a Pairwise Chi-Square Test for QVOA.
910 Summary data for ABT-199 tested at **(C)** 1μM and **(D)** 100nM in following HIVE assays. Levels of HIV
911 DNA (left) and IUPM (right) are shown, comparing ABT-199 alone vs NoTx, and Bryostatin-1+ABT-199
912 vs Bryostatin-1 (n=8 for C, n=6 for D). Dashed lines indicate paired Bryostain-1 vs NoTx conditions.
913 DMSO was added to NoTx conditions at a matched concentration with +Tx conditions. Statistical
914 significance was determined by Wilcoxon matched-pairs signed rank test.

Figure 6

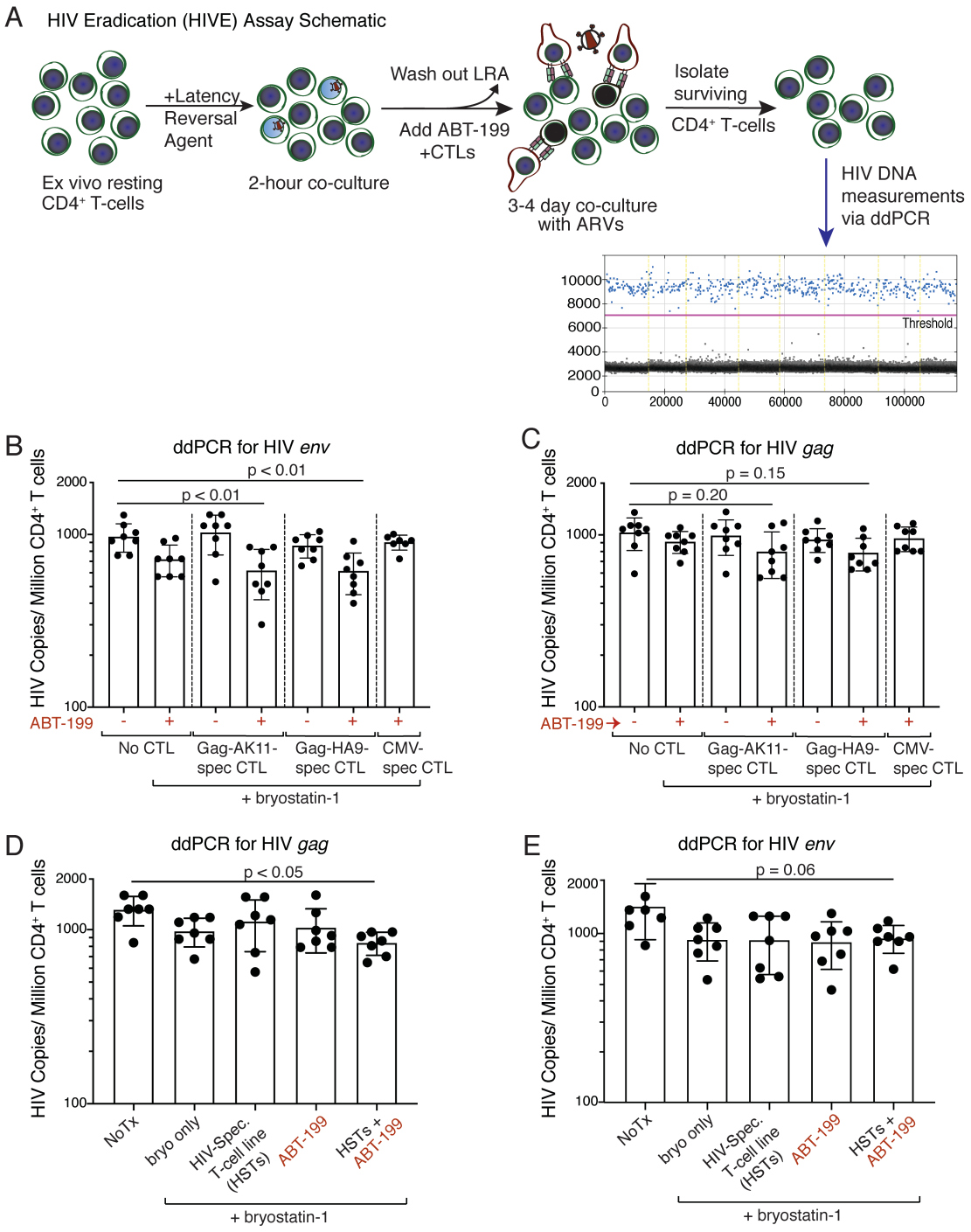

Fig. 6. ABT-199 enables modest reductions in HIV-infected cells by HIV-specific T-cell effectors, following reactivation with bryostatin-1. (A) Schematic of the HIV Eradication (HIVE) assay with droplet digital PCR as the endpoint. (**B-E**) ddPCR data measuring HIV-*env* (**B&E**) or HIV-*gag* (**C&D**) in DNA from HIVE assay samples, as indicated. Shown are mean ± SD values of 8 replicates per samples

(following exclusion of outliers based on pre-specified criteria, see Methods). P values were calculated by Ordinary one-way ANOVA, with Tukey's multiple comparisons test if ANOVA test was significant.

Figure 7

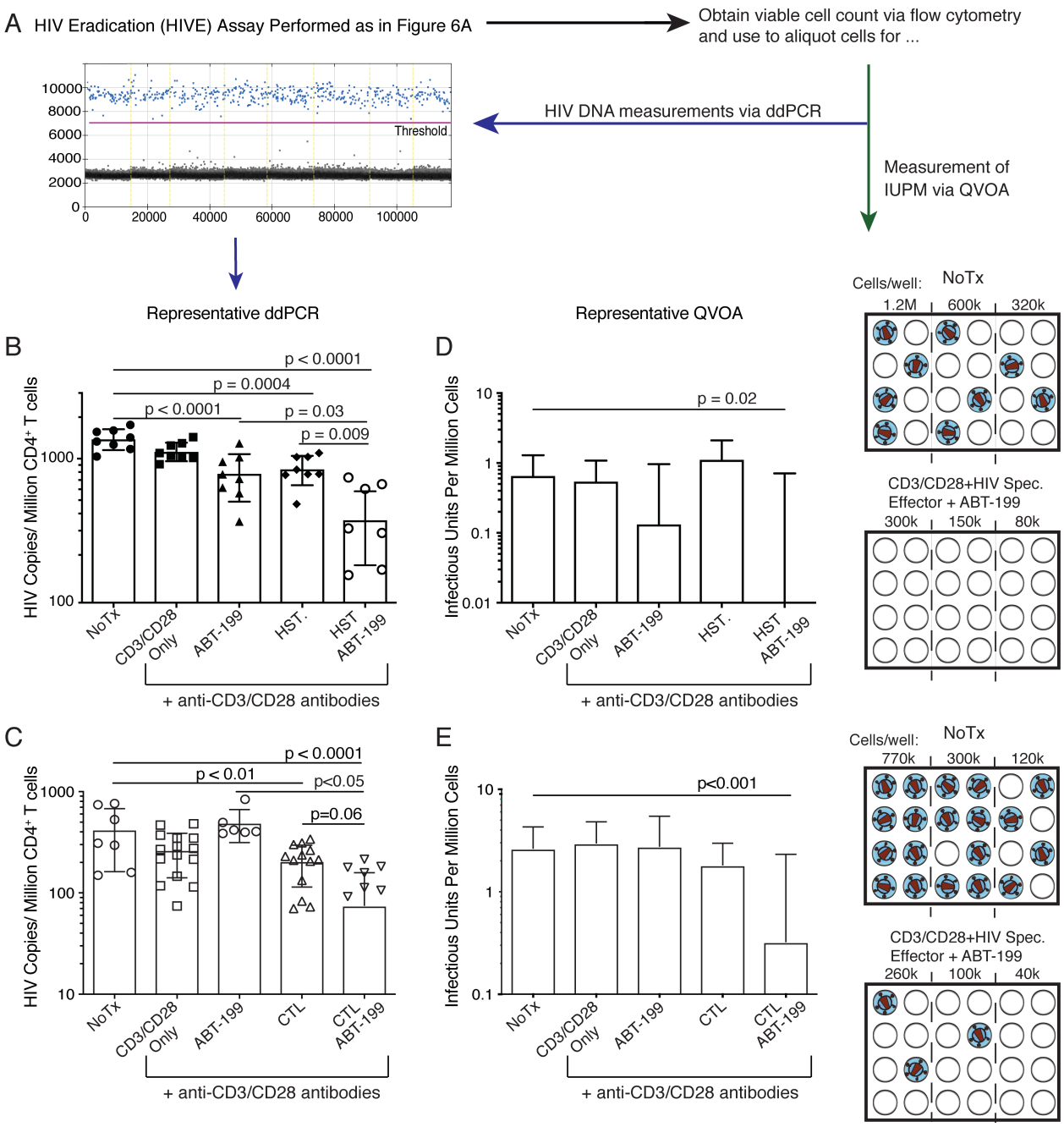

Fig. 7. ABT-199 enables CTL-mediated reductions in *ex vivo* HIV reservoirs following reactivation with anti-CD3/anti-CD28. (A) Schematic of the HIV Eradication (HIVE) assay showing representative endpoints. **(B, C)** Representative ddPCR data (mean ± SD of 8-12 replicates) from two HIVE assays using: autologous HSTs in **(B)**, and an autologous HIV-specific CTL clone in **(C)**. P values are determined by one-way ANOVA test. **(D, E)** Representative QVOA data showing maximum likelihood estimates of IUPM

± 95% confidence intervals (the same HIVE assays in B, C). P values are determined by pairwise chi-square test. The representative QVOA plates shown on the right correspond to the NoTx and the anti-CD3/anti-CD28+HIV-spec. effector+ABT-199 conditions.

Figure 8

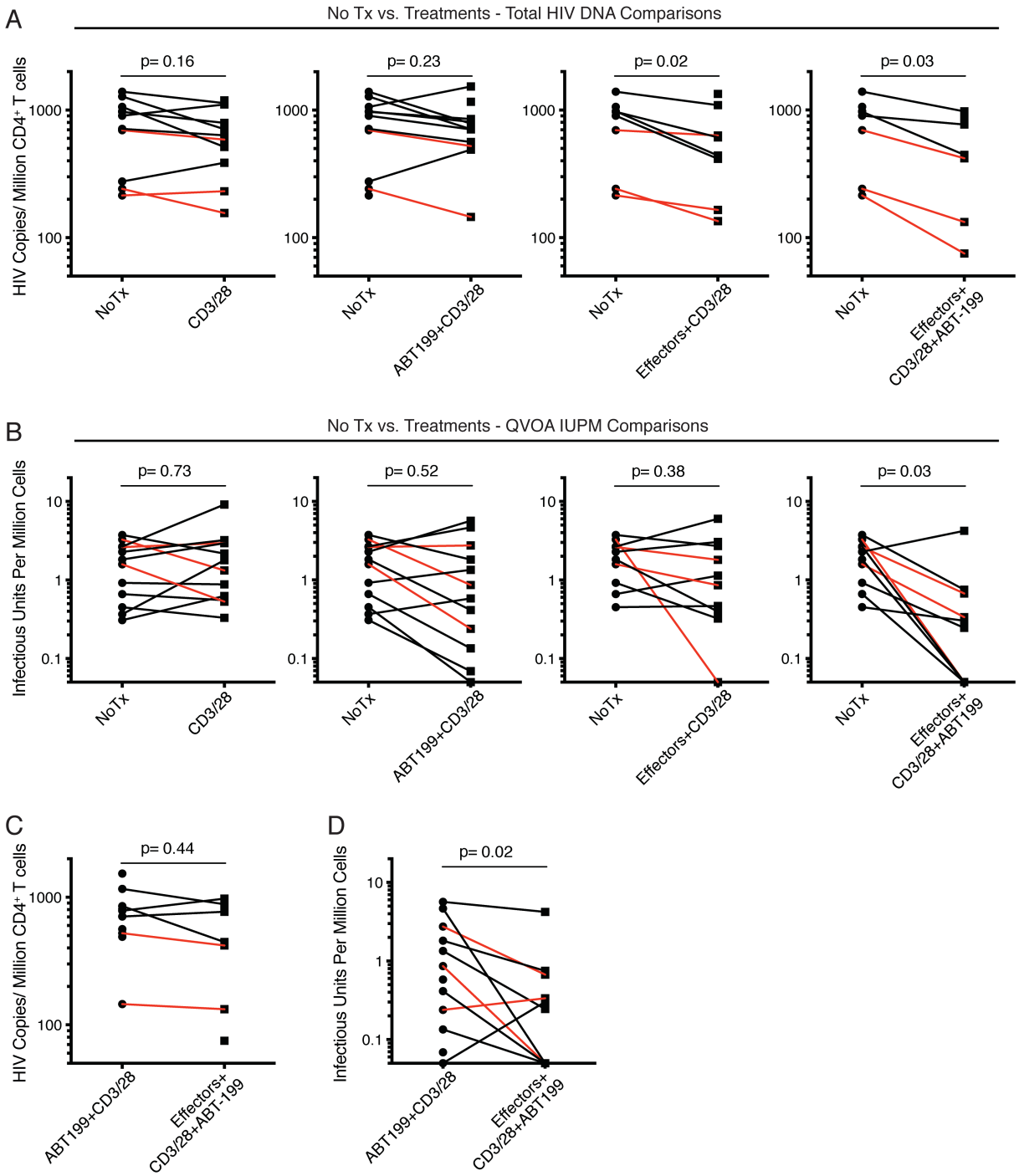

933

934 **Fig. 8. Summary data showing that tri-combinations reduce *ex vivo* HIV reservoirs. (A)** Summary

935 ddPCR data for HIV DNA levels following HIVE assays, comparing each of the indicated treatment

936 conditions. (n=10, except for anti-CD3/anti-CD28+HIV-Spec. effector+ABT-199 n=6 due to insufficient

cell numbers). **(B)** Summary QVOA data quantifying IUPM following HIVE assays, comparing each of the indicated treatment conditions (n=10). **(C)** Summary ddPCR for HIV DNA and **(D)** QVOA data quantifying IUPM comparing anti-CD3/anti-CD28+ABT-199 vs anti-CD3/anti-CD28+HIV-Spec. effector+ABT-199, emphasizing the reduction of IUPM is only seen in combination of all three compounds (n=6 for C and n=10 for D). Lines in red indicate where autologous HIV-specific CTL clones were used, black lines were HSTs. Statistical significance was determined by Wilcoxon matched-pairs signed rank test.

Table 1. ART-Suppressed Participant Clinical Data

Participant ID	Gender	Age (y)	Ethnicity	ART regimen	Duration of Viral Load undetectable (month)	Viral Load (Copies/mL)	Est. time between infection and ART (months)
OM5011	M	46	White	3TC/ABC/DTG	133	<50	38
OM5267	M	28	White	3TC/ABC/Ral	91	<50	4
OM5334	M	34	White	Genvoya/Edurant	63	<50	2
OM5148	M	48	White	3TC/ABC/NVP	149	<50	57
OM5365	M	58	White	Kivexa/tmc114/rtv/tmc125/integrase/maraviroc	114	<50	18
OM5162	M	56	White	truvada/integrase/kaletra	162	<50	3
OM5220	M	54	White	3TC/ABC/DTG	102	<50	Unknown
WWH-B004	F	63	White	DTG+MVC*	~169	<50	<12
WWH-B008	M	64	Black	Descovy/Truvada	~47	<50	~60
WWH-B011	M	55	White	Odesfy	~76	<50	~264
WWH-B012	F	52	White	Odesfy	~98	<50	<12

Table 2. ART-Naïve Participant Clinical Data

Participant ID	Gender	Age(y)	Viral Load (copies/mL)	CD4 counts Cells/mm^3	HIV dx year	ART Status	Visit 1 (year)
B465	M	47	61,830	352	2012	naïve	2017
B461	M	49	42,620	333	2012	naïve	2017
B411	F	58	6,690	877	2004	naïve	2017
OM5374	M	29	96,125	214	2018	naïve	2018